Thermal Degradation Behavior of Sewage Sludge in Pyrolysis Processes

By

Rumaisa Tariq

School of Chemical and Materials Engineering

National University of Sciences and Technology

2018

Thermal Degradation Behavior of Sewage Sludge in Pyrolysis Processes

Name: Rumaisa Tariq

Reg. No: 00000118912

This thesis is submitted as a partial fulfillment of the requirements for the degree of

MS in Chemical Engineering

Supervisor Name: Dr. Salman Raza Naqvi

School of Chemical and Materials Engineering (SCME)
National University of Sciences and Technology (NUST)
H-12 Islamabad, Pakistan
February 2018

Dedication

This thesis is dedicated to my lovable parents "Mr. Muhammad Tariq Hassan and Mrs. Rubina Tariq" who provided me support and confidence to face the difficulties of life and courage to fulfil my dreams.

Acknowledgments

All respect to the "**ALLAH ALMIGHTY"** who made me able to reflect, research and blessed me with the strengths to complete my MS project within the optimum required standards. May the Peace be upon **"HAZRAT MUHAMMAD (S.A.W)"** and his entire kin. The source of knowledge and blessings for the entire humanity and the universe.

I desire, to express my sincere thanks to my Supervisor **Dr. Salman Raza Naqvi,** who being a mentor provided me a constant guidance and support that empowered me to finish this work within due course of time. His supervision assisted me in all the dimensions of this thesis work. I could not have anticipated having a better advisor for my MS research. He inspired and encouraged me throughout my journey in bringing this assigned task to an adequate completion.

I am also obliged to **Dr. Bilal Khan Niazi** and **Dr. Tayyaba Noor** Assistant Professor in SCME NUST for the unremitting assistance, treasured guidance and recommendations in the technical and experimental work.

I am extremely thankful to, Dean/Principal of SCME **Dr. Arshad Hussain** and H.O.D Chemical Engineering **Dr. Abdul Qadeer Malik** for providing me with all the vital facilities and the commendable atmosphere for the research.

My truthful thanks to **All Lab Engineers** who rendered every possible assistance in laboratory analysis pertaining to this task within the most befitting manner.

Good Friends are blessing of God, Gratitude is extended to my friends and Co-researcher Ayesha, Saba, Memoona, Humaira and Zeeshan. At the conclusion, I would mention with an immense pride and internal satisfaction, the unconditional love, support and constant motivation through thick in thin my beloved family and friends bestowed upon me during this journey. For sure, without a doubt I am absolutely nothing without the tap on the back and positive reception from them.

Abstract

By considering the growing energy demand internationally, it is necessary to highlight alternate renewable and sustainable resources of fuel such as biomass and domestic waste to produce energy by unconventional methods. Non-lignocellulosic biomass like sewage sludge is the most suitable alternative used instead of fossil fuels because this material has potential to produce both bio-oil and biochar. The current research emphasis on the pyrolysis process of sewage sludge to study the thermal degradation behavior through thermogravimetric analysis and by using lab scale reactor (autoclave pyrolyzer unit) to obtain useful products. Elemental composition of sewage Sludge is determined by ultimate and proximate analysis and existed functional group is identified through FTIR analysis. The Effect of heating rate (5°C/min, 10°C/min and 20°C/min) on thermal degradation behavior is studied by TGA-DTA technique in Nitrogen atmosphere and found the main degradation phase between 200-600°C which is further divided into two phases one from 200-400°C and 400-600°C for the thermal disintegration of different components. The kinetic and thermodynamic parameters are calculated by using model fitting kinetics such as Coats and Redfern method and model free kinetics such as Friedman, KAS, OFW and Popescu is done to describe pyrolysis behavior of sewage sludge by using TGA-DTA data. The effect of temperature (350°C, 400°C and 450°C) is studied through autoclave pyrolyzer unit by keep feedstock, pressure and agitation conditions constant. In lab scale pyrolysis process, highest bio-oil yield was achieved at 450°C. The products such as bio-oil, char and gases are further analyzed by GC-MS, FTIR, TGA and GC-TCD. GC-MS peak area percentage showed that the bio-oil exhibited variety of chemical groups such as acids, carbonyls, furans, phenols, sugars and aromatic hydrocarbon. GC-TCD showed area percentage of methane and carbon dioxide also increased as the temperature increased and area percentage of hydrogen decreased as temperature increased. Various functional group is identified present in char produced at different temperature through Fourier transform infrared spectroscopy.

Table of Contents

Dedication i
Acknowledgments ii
Abstract iii
List of Figures vii
List of Tables viii
Acronyms ix
Chapter 1 1
Introduction 1
1.1 Background: 1
1.2 Production of Sewage Sludge: 1
1.3 Sewage Sludge as a Source of Renewable fuel: 3
1.4 Pyrolysis of Sewage Sludge: 3
1.4.1 Mechanism of Pyrolysis: 3
1.4.2 Analytical Pyrolysis: 5
1.5 Problem Statement: 6
1.6 Research Objective: 7
1.7 Scope of Study: 7
1.8 Chapter Summary 8
Chapter 2 9
Literature Survey 9
2.1 Introduction 9
2.2 Source and Properties of Sewage Sludge: 9
2.3 Thermal degradation characteristics of sewage sludge: 14
2.4 Poly-generation and application of Pyrolysis: 17
2.5 Kinetic Models: 20
Chapter 3 23
Material and Methodology 23
3.1 Raw Material: 23
3.2 Characterization of Sewage Sludge: 24
3.2.1 Proximate Analysis of Sewage Sludge: 24
3.2.2 Ultimate Analysis of Sewage Sludge: 25
3.2.3 FTIR of Sewage Sludge: 26

3.3 Thermal Degradation Behavior of sewage sludge through TGA:..... 27
3.4 Kinetic Analysis: 28
3.4.1 Fundamental Kinetic Expressions: 28
3.4.2 Model Fitting Approach: 29
3.4.3 Model Free Approach 30
3.5 Thermodynamic Analysis: 31
3.6 Thermal Degradation Behavior through Autoclave Pyrolyzer Unit: 32
3.7 Characterization of pyrolysis Products: 34
3.7.1 Gas chromatography–mass spectrometry (GC–MS) of Liquid Oil: 34
3.7.2 Infrared spectroscopy (FTIR) of Char: 35
3.7.3 Thermogravimetric Analysis (TGA) of Char:..... 35
3.7.4 Gas Chromatography with TCD detector of Gaseous Product: 35
Chapter 4 37
Result and Discussion 37
4.1 Characterization of Sewage Sludge:..... 37
4.1.1 Proximate Analysis of Sewage Sludge..... 37
4.1.2 Ultimate Analysis of Sewage Sludge: 38
4.1.3 Fourier Transform Infrared Spectroscopy (FTIR): 39
4.2 Thermal degradation Behavior of Sewage Sludge through TGA: 40
4.2.1 TGA of Sewage Sludge: 40
4.2.2 DTA of Sewage Sludge: 41
4.3 Kinetic and Thermodynamic Analysis through Model Fitting Approach: 42
4.3.1 Kinetic Parameters through Coats and Redfern Method: 42
4.3.2 Thermodynamic Parameters through Coats and Redfern Method:..... 48
4.4 Kinetic and Thermodynamic Analysis through Model Free Approach: 53
4.4.1 Kinetic Parameters through Friedman, KAS, OFW and Popescu Method: 53
4.4.2 Thermodynamic Parameters through Friedman, KAS, OFW and Popescu Method 60
4.5 Sewage Sludge Pyrolysis in an Autoclave Reactor:..... 64
4.6 Oil Analysis Through GC-MS:..... 65
4.7 Gas Analysis Through GC-TCD:..... 70
4.8 Thermogravimetric Analysis of Char:..... 72
4.8.1 TGA of Char:..... 72
4.8.2 DTA of Char:..... 73
4.9 FTIR Analysis of Char:..... 74
Chapter 5 76

Conclusion and Future Recommendation 76
5.1 Conclusion:..... 76
5.2 Future Recommendations: 77
References:..... 78

List of Figures

Figure 1.1: World Annual production of sewage sludge [5]---------- 2
Figure 1.2: Schematic diagram of mechanism of sewage sludge pyrolysis [14] ------ 4
Figure 3.1: Drying and size reduction of sewage sludge---------- 23
Figure 3.2: Initial and final form of sewage sludge after proximate analysis --------- 25
Figure 3.3: CHNS elemental analyzer (PerkinElmer 2400II, USA)---------- 25
Figure 3.4: Working principal of Fourier transform infrared spectroscopy [96].----- 26
Figure 3.5: Working principal of TGA [97] ---------- 27
Figure 3.6: Original diagram of autoclave pyrolyzer unit---------- 33
Figure 3.7: Block diagram of autoclave pyrolyzer unit ---------- 33
Figure 3.8: GC-MS SHIMADZU QP 2020 with HP 5973 quadrupole detector------ 34
Figure 3.9: SHIMADZU GC-2010 plus gas chromatograph with TCD detector----- 36
Figure 4.1: Percentage components of sewage sludge through proximate analysis -- 37
Figure 4.2: Percentage Component of sewage sludge through ultimate analysis----- 38
Figure 4.3: FTIR of sewage sludge sample obtained from municipal waste water treatment plant---------- 40
Figure 4.4: TGA of sewage sludge sample at 5, 10 and 20 °C/min ---------- 41
Figure 4.5: DTA of Sewage sludge sample at 5, 10, 20°C/min ---------- 42
Figure 4.6: Typical linear regression lines of model free method ---------- 54
Figure 4.7: Activation energy as a function of conversion.The trends of Ea derived from different iso-conversional methods are presented in this figure ---------- 59
Figure 4.8: Liquid, solid and gaseous products obtained from pyrolysis of sewage sludge through autoclave pyrolyzer unit---------- 65
Figure 4.9: Effect of temperature on area percentage % of different gases analyzed by GC-TCD---------- 71
Figure 4.10: TGA curves of pure sewage sludge, char 1 obtained at 350°C, Char 2 obtained at 400°C, AND CHAR 3 Obtained at 450°C ---------- 72
Figure 4.11:DTA curves of pure sewage sludge, char 1 obtained at 350°C, char 2 obtained at 400°C, char 3 obtained at 450°C---------- 74
Figure 4.12: FTIR curves of pure sewage sludge, char 1 obtained at 350°C, char 2 obtained at 400°C, char 3 obtained at 450°C---------- 75

List of Tables

Table 1.1: Amount of sewage sludge production per day in different countries 2
Table 2.1: Source and Composition pf waste water sewage sludge 11
Table 2.2: Investigation on thermal behaviors of sewage sludge using TGA 15
Table 2.3: Investigation on thermal behaviors of sewage sludge using TGA 18
Table 2.4: TGA pyrolysis for kinetic studies for sewage sludge 21
Table 3.1: Specific condition and equipment used in proximate analysis 24
Table 3.2: Kinetic model name with their respective g(a) 29
Table 4.1: Kinetic parameters of sewage sludge sample by using different mechanism function for model fitting approach 44
Table 4.2: Thermodynamic parameters of sewage sludge sample at 5, 10, and 20°C/min from Model Fitting Approach. 50
Table 4.3: Kinetic Parameters Through Model Free Approach. 55
Table 4.4: Thermodynamic parameters of all four method with conversion. 60
Table 4.5: Yield of liquid, solid and gas product obtained from sewage sludge pyrolysis at different temperature 64
Table 4.6: List of Identified components and their area percentage through GC-MS of pyrolysis liquid oil obtained at 350°C, 400°C and 450°C 67
Table 4.7: Classification according to area percentage of the different functional group of compounds in the chromatographed elements of the pyrolysis oils at different temperature 70
Table 4.8: Classification according to area percentage of the different gases present in pyrolysis gas obtained at different temperature. 71

Acronyms

ABBREVIATIONS

MJ	Mega Joules
Kg DM	Kilogram per Cubic Decimeter
GHS	Green House Gas
SS	Sewage Sludge
FTIR	Fourier Transform Infrared Spectroscopy
GC-MS	Gas Chromatography Mass Spectrometry
TGA	Thermogravimetric Analysis
DTA	Differential Thermogravimetric Analysis
DSC	Differential Scanning Calorimetry
CHO	Carbon, hydrogen, and oxygen (wt%)
GC-TCD	Gas chromatography with thermal conductivity detector
FWO	Flynn-Wall-Ozawa
KAS	Kissinger-Akahira-Sunose
HV	Heating Value
M	Moisture
VM	Volatile Matters
FC	Fixed Carbon
Extr.	Extractives

SYMBOLS

C	Carbon
H	Hydrogen
N	Nitrogen
O	Oxygen
S	Sulfur
M	Moisture %
VM	Volatile Matter %
FC	Fixed Carbon%
Extr.	Extractive
R	Universal gas constant
T	Temperature

U	Gas flow rate
t	Time
α	Degree of conversion
f(α)	Conversion function
g(α)	Kinetic function
m	Mass of substrate
m_i	Initial substrate mass
m_f	Final mass of solid
E_a	Activation Energy
A	Pre-exponential Factor
β	Heating rate
Exp	Exponential
dα/dt	Rate of isothermal process
dt/dT	Inverse of the heating rate
dα/dT	Non-isothermal reaction rate
n	number of orders

Chapter 1

Introduction

1.1 Background:

The requirement of energy is being enlarged by using alternative way because of speedy intensification in worth and exhaustion of fossil fuels beyond the limits. By utilizing these fossil fuels, the volume of CO_2 in the troposphere can be amplified due to larger greenhouse gas (GHG) emissions which consequences in unadorned global warming. Other than this reason that these fuels have restricted reserves, the exploitation of fossil fuels energy can be a root of frequent atmospheric concerns such as greenhouse effect, depletion of ozone layer, acid rain and other pollutions. More extremely, the carbon dioxide originated through fossil fuels subsidizes 84% of GHG unconfined to the troposphere[1]. By considering the intensified energy mandate transnationally, it is obligatory to spot out substitute renewable and sustainable resources of fuel such as different wastes and lignocellulosic biomass to obtain energy by eccentric methods, which can assist to diminution carbon footprints these resources have gained attained concentration during the preceding eras.

Non-lignocellulosic biomass like sewage sludge is the most suitable alternative used instead of fossil fuels this material has potential to produce both bio-oil and biochar. Sewage sludge can provide energy and fuel by thermochemical conversion so this is considered as most promising alternate technology to reduce the amount of waste and harmful environmental impact.

1.2 Production of Sewage Sludge:

Table 1.1 demonstrated statistics about the quantity of sewage sludge production in several republics projected by European state in year 2014 and reorganized in year 2016. The amount of sewage sludge production is largely depending upon level and method of treatment applied to waste water, population growth and volume of wastewater stream. Christodoulou et al. provided the information of annual production of sewage sludge in different countries in 2016 is shown in the figure 1.1.

Table 1.1: Amount of sewage sludge production per day in different countries [2][3][4]

Country Name	Amount of SS production/day
Germany	1815500 tons
Ireland	64600 tons
France	886500 tons
Poland	540300 tons
Finland	141200 tons
UK	1136700 tons
China	95890.41 tons
Switzerland	194500 tons

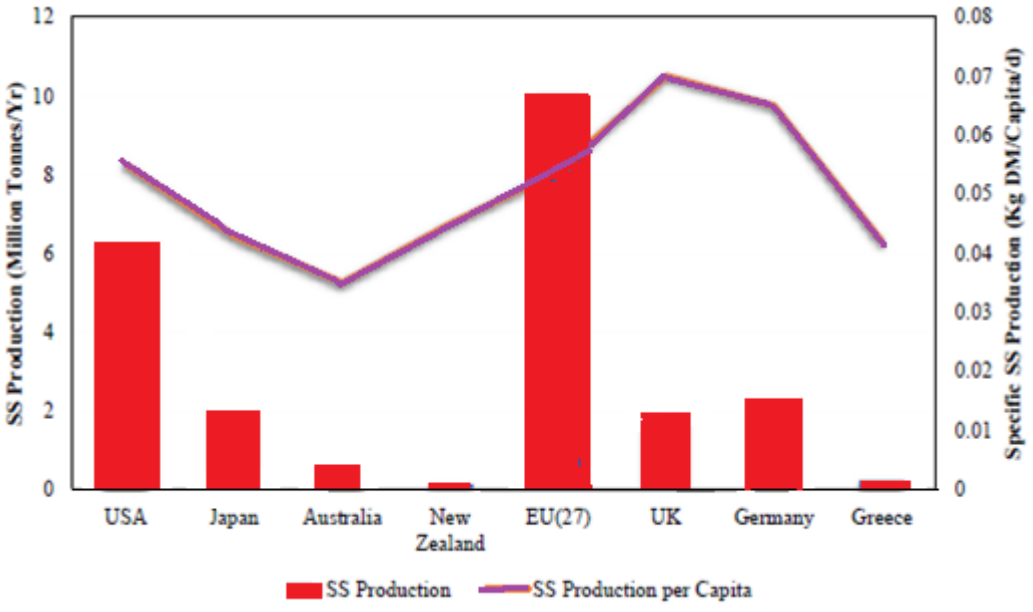

Figure 1.1: World Annual production of sewage sludge [5]

1.3 Sewage Sludge as a Source of Renewable fuel:

Sewage sludge is strong waste or leftover blend of proteins, starches, lipids or fats, natural and inorganic issues. With the extensive advancement of ventures and expanding populace, the generation of sewage slime is definitely expanded which can cause natural and monetary issues in regard to air, water and soil contamination because of essence of lethal and unsafe substance in sewage ooze, for example, microorganisms, infections, dioxin, non-biodegradable natural mixes, substantial metals et cetera. In spite of the fact that sewage swill can be utilized for vitality source since it can possibly deliver bio energizes by utilizing thermochemical change procedures and this can likewise limit the unsafe natural effect. Dry type of sewage sludge can be utilized as inexhaustible fuel because of high calorific esteem and sensible unstable substance as that of dark colored coal [6]. As indicated by Fytili et al. dried sewage has unpredictable substance 30−88% and calorific esteem normally 11−25.5MJ/kg [7]. The utilization of sewage sludge as sustainable power source assets is taken as healthier choice since this source can give around 10% of worldwide vitality stock [8].

1.4 Pyrolysis of Sewage Sludge:

1.4.1 Mechanism of Pyrolysis:

Pyrolysis is a procedure of altering diverse form of sewage sludge in the disappearance of air or oxygen to generate three categories of product based on their nature, namely, solid char, liquid oil and volatile gas components by thermal deprivation method. Pyrolysis process starts with the formation of vapors of volatile components then primary disintegration of non-volatile substance occurs to produce char, tar and gases. Then with the increasing temperature secondary decomposition of char occur to produce hydrocarbons and benzene derived compounds in the gas form [9]. A schematic demonstration of sewage sludge pyrolysis mechanism is given in Figure 1.2

With the temperature increase, the fuel gas having higher percentage of hydrogen produces because dehydrogenation reactions de-carbonization of oxygenated hydrocarbons can increase in H_2 content that comes from substantial hydrocarbon compounds. These rejoinders suppressed the cracking reactions which promote the polymerization and poly-condensation reactions to occur. Moreover, H_2 can be act as upright pointer for the secondary cracking of tars to reduce the amount of it [10][11].

Menéndez et al. concluded that CO and CO_2 produces at the temperature range of lower than 450°C by the breaking of carbonyl and carboxyl functional groups of sewage sludge. CO is the main secondary product obtained from cracking tar at higher temperatures[12]. Furthermore, hydrocarbon compounds are also degrading at elevated temperatures, as shown in reaction below:

$$C_2H_6 \rightarrow C_2H_4 + H_2 \qquad 1.1$$

$$C_2H_4 \rightarrow CH_4 + C \qquad 1.2$$

The main analysis of tar recommended that the main mechanism of the disintegration of aliphatic acids occur through esterification reaction and the breakage of peptide linkage in proteins through contagious components present inside sewage sludge. Consequently, large amount of amide and nitrile compounds containing groups are present in oil obtaining from pyrolysis of sewage sludge. Morf et al. told in their article that polyaromatic hydrocarbons are formed due to presence of phenol derivatives in the sewage sludge and the formation of naphthalene occur due to original phenol in the sludge[13].

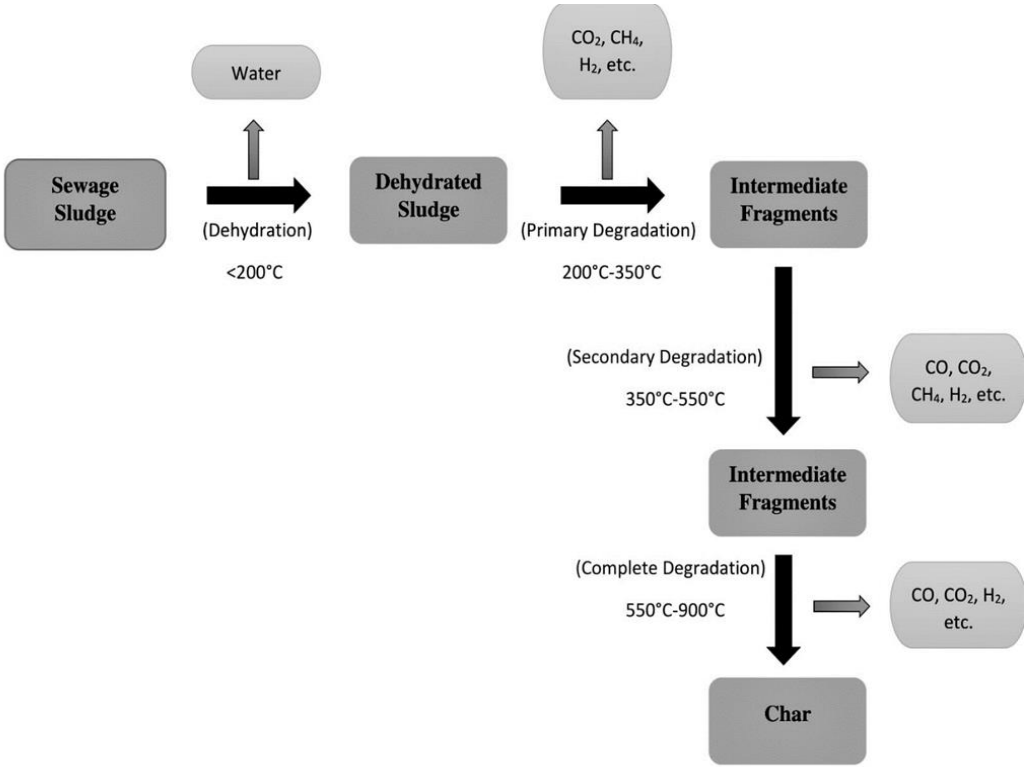

Figure 1.2: Schematic diagram of mechanism of sewage sludge pyrolysis [14]

The complete mechanism of pyrolysis cannot be explained fully particularly in the situation of damp sewage sludge. Damp sludge has higher percentage of moisture content which increases the steam vapors releases at high temperatures due to this reason more endothermic reactions occur between the steam and pyrolysis products and H_2 production increases[15]. Some steam vapors can be converted into liquid fraction by condensation reaction and then the water gas shift and the steam reforming reactions occur to convert remaining components and production of H_2 content occur[16]. At last the amount of gas produced by secondary tar cracking at elevated temperatures. By the devolatilization of the hydrocarbons solid char produced at high temperature by reaction occur between the intermediate products formed during pyrolysis[17].

1.4.2 Analytical Pyrolysis:

Analytical pyrolysis is to study the pyrolysis behavior by using different analytical tools like thermogravimetric analyzer TGA, differential gravimetric analyzer DTA and gas chromatography online attached with mass spectrometry GC-MS. These analytical pyrolysis techniques are usually used to find out the thermal degradation behavior during pyrolysis and configuration of non-condensable gases. In all analytical pyrolysis, usually mass loss happens in three steps, centered around 350°C, 450°C or 550°C, by producing large amount of pyrolysis products[18].

TGA is to a thermogravimetric analysis technique whose working principle is a controlled temperature program used to measure the weight of a sample continuously. The physical and chemical properties of sample based on variation of sample weight with respect to time and temperature can be obtained by using the differential thermogravimetric (DTG) curve resulted from differential of TGA curve [19]. The usage of thermogravimetric analyzer has a lot of advantages like it requires minimum amount of feedstock, due to programed based technique its operation is easy, accurate and precise record of temperature and percentage of weight loss. TGA system can be helpful in defining proximate analysis of sewage sludge and to figure out the thermal physiognomies like ignition and exhaustion points and chemical kinetics of sewage sludge by using different techniques like combustion, torrefaction, pyrolysis, gasification [20][21].

Presently, TGA, DTA and DSC techniques are able to give thermal degradation and kinetic evaluation of solid fuel. These evaluations are very important to find out the reactivity and thermal ability of burning material. These techniques can be used to evaluate the kinetic parameters under isothermal and non-isothermal conditions. TGA can be able to suggest the thermal deprivation outlines of sewage sludge and char obtained from either hydro treatment or bio treatment underneath air or inert atmosphere for subsequent kinetic investigation. The configurations explain the consequence of heating rate, properties of sludge, stability and compatibility of sewage sludge to progression [22]. Several types of kinetic methods exist that are based on the thermal statistics for assessment and development. The foremost guidelines of these kinetic evaluations for thermal investigation are boundaries and analytical records. They are mutually obtained from analogous experiment and conducted in very limited time [23][24].

1.5 Problem Statement:

The complete conventional and unconventional pyrolysis of dried sewage sludge attained as of waste water treatment plant produced bio-oil, bio-char and gaseous product. Fuels and energy production from dried sewage sludge through analytical pyrolysis and their physiochemical properties assessment for eco-friendly application is still not sightseen completely[25]. Low quality bio-fuels are produced directly from the pyrolysis process due to acidic and oxygenated nature because the presence of materials such as phenols, aldehydes, ketonic and acidic components and furans[26]. It is compulsory to recover excellent properties related to bio-fuels comparable to hydrocarbons fuel by engaging upgrading techniques[27]. Pyrolysis through autoclave pyrolyzer unit is one of the finest substitute way used to convert various oxygenated compounds into required supplies such as benzene, toluene, xylene and naphthalene.

To demonstrate enough the characteristics of sewage sludge pyrolysis, the detailed approximation of kinetic and thermodynamic constraints of non-catalytic sewage sludge pyrolysis is vital for the considerate and modelling of pyrolysis process at industrial scale. Comprehensive work on thermodynamic and chemical kinetics of sewage sludge pyrolysis by using TGA data seems like to be insufficient. So, this project has comprehended resolution to convey a detail description of pyrolysis process surroundings, thermodynamic and kinetics constraints by using sewage sludge

obtained from municipal waste water treatment plants. A multiplicity of models such as Friedman, KAS, OFW and Coats & Redfern models can be used to inspect the thermal disintegration performances of sewage sludge will be exemplified.

1.6 Research Objective:

To report the current challenges in sewage sludge pyrolysis, this thesis work inspects the analytical and non-catalytic pyrolysis of dried sewage sludge for bio-fuels production. The inclusive research objective is to produce and characterize the biofuels from sludge pyrolysis and performance evaluation of pyrolysis process by different kinetic models. The following assessable objectives are under taken in the present study.

- To collect and characterize the domestic wastewater sewage sludge to explore the physiochemical properties
- To study the influence of pyrolysis temperature of sewage sludge using lab scale reactor and characterize the products
- To investigate the sewage sludge pyrolysis behavior using thermogravimetric analysis
- To determine the kinetic parameters of sewage sludge pyrolysis process using model-free and model-fitting methods
- To determine the thermodynamic parameters of sewage sludge pyrolysis process using model-free and model fitting methods.

1.7 Scope of Study:

The research work primarily emphases on the study of non-catalytic and analytical pyrolysis of dried sewage sludge for oil production, gas and char product. For understanding the thermal degradation behaviour thermogravimetric analysis technique is employed.

Sewage Sludge was collected from a municipal waste water treatment plant and size reduction was occurred by using ball mill. To comprehend the properties of the sewage sludge, proximate, ultimate and FTIR analysis were performed to achieve the essential knowledge about the physicochemical properties of sewage sludge.

Powdered form dried sewage sludge is experimented to investigate the behaviour of pyrolysis process of sewage sludge in autoclave pyrolyzer unit to produced bio-oil.

Characterization techniques such as GC-MS, GC-TCD, FTIR and TGA analysis are carried out to find out the composition and characterization of products.

This study presents the kinetic study on analytical pyrolysis of dried sewage sludge. Model free method such as Friedman, KAS, OFW, Popescu and model fitting models such as Coats and Redfern method were used to construe the thermogravimetric data attained through pyrolysis process. Numerous reaction models are existing in the Coats and Redfern Models which is also used in this study.

This work investigates the thermodynamic parameters based on analytical pyrolysis of dried sewage sludge. Model free method such as Friedman, KAS, OFW, Popescu and model fitting models such as Coats and Redfern models were used to infer the thermogravimetric data gained from the pyrolysis process. Many reaction models are accessible in the Coats and Redfern Models which is also used in this study the thermodynamic parameters.

1.8 Chapter Summary

This manuscript contains of five sections. The contacts of each section are specified in the following passages.

- **Chapter 1** delivers need of proposed topic, contextual and existing issues related to the topic. It also clarifies the definite terms, process, problem statement, objectives and scope of the strategic research work.
- **Chapter 2** will draft the literature survey accomplished to describe preceding efforts done on the thermal degradation of sewage sludge obtained from various sources. It also comprises surveys based on source and properties of sewage sludge and various pyrolysis techniques.
- **Chapter 3** contains the methodology associated to the sample preparation and characterization, pyrolysis inquiry work and kinetic and thermodynamic analysis. It will also provide the related information about procedure and apparatus contributing in the experimental investigations.
- **Chapter 4** delivers results and discussions. The material characterization, experimental, kinetic and thermodynamic modelling consequences are existed and explained based on various point of view.
- **Chapter 5** contains all the findings and conclusions in the existing learning and delivers the upcoming endorsements for the related work.

Chapter 2

Literature Survey

2.1 Introduction

This current section evaluates origin, elemental and chemical composition of sewage sludge and thermal deration of sewage sludge through conventional methods and through TGA to yield bio-oil, char and gas products. A brief survey on past work related to kinetic analysis of sewage sludge based on thermogravimetric data is also presented in this section to investigate the thermal disintegration of pyrolysis behavior. Literature related to real world methods for poly-generation and their applications are also listed in this chapter.

2.2 Source and Properties of Sewage Sludge:

Real wellspring of sewage sludge is metropolitan waste water treatment plants. Sewage sludge has ability to acquire by mechanical waste water streams. Sewage slop has diversity from various biomass sources in either basic or synthetic arrangement. Essentially, Sewage slop is intricated blend of nearly natural, nonorganic materials and moisture [28]. Samolada et al. discover that sewage slop additionally contains some problematic materials like overwhelming metals, natural poisons and pathogens [29]. Xie et al. expressed that the dehydrated slime, acquired through city squander water treatment plant contains 13.8%-17.9% natural substance [30]. Inoue et al. portrayed that dehydrated sewage slime comprises very nearly 12.4% natural substance and 3.8% fiery debris element [31]. Sewage Sludge contains variable synthetic creation for the most part because of various ecological conditions, area, generation strategies, sort of sewage slime, root of the waste stream, the sanitization dealing of wastewater, the adjustment handling of the sewage slop, the stretch and capacity states of the sewage sludge [32].

Table 2.1 depicts the current survey on the essential and synthetic structure of sewage muck acquired from squander water treatment plants. The natural and substance creation from sewage slop can be computed by utilizing extreme and proximate investigation. A definitive examination is natural investigation to discover the level of gas present such as nitrogen, sulfur, carbon, oxygen and hydrogen, proximate investigation for discovering level of dampness, unpredictable issue, settled carbon and ash [33]. As per extreme investigation sewage slime comprises higher level of nitrogen percentage as compared to in cellulosic biomass. It originates through protein sections and support its utilization in compost [34]. Proximate investigation uncovers fact that sewage slime contains greater slag as compared to in lignocellulosic biomass and examination reveals, fiery debris evacuation framework ought to be introduced with container even though utilizing such sort of material. The fiery debris got by pyrolysis of sewage slime consists of mineral deposits, for example, quartz or calcite and essential investigation deliver data that minerals made up from various level of Fe, Ca, Mg and K which can assist in boosting pyrolysis response. Substantial metals like Cr, Ni, Co, Hg, Cd, Pb and Zn additionally exhibit in sewage sludge [35].

Heating value is additional imperative constraint whose esteem has in charge of the most extreme and least level of item. Heating value could be examined by test setup or by utilizing basic lab scale tests like bomb calorimeter. Formulas and correlations also dictated these values [36]. Value estimation of test primarily relies on the dampness content. At the point when dampness substance and fiery remains content is lower, warming esteems winds up noticeably more prominent. The higher heating estimation of dehydrated sewage slime has extended from 8-17 MJ/kg. To keep up reasonable comprehension of pyrolysis of sewage slop, it has importance to consider compound synthesis and properties of sewage muck and incredibly influence the result of pyrolysis [37].

Table 2.1: Source and Composition pf waste water sewage sludge

Year	Sample	Proximate Analysis				Ultimate Analysis					HV	Biochemical Composition		Ref.
		Moisture wt.%	Volatiles wt.%	Fixed Carbon wt.%	Ash wt. %	C%	H%	N%	S%	O%	MJ/kg	Protein	Extr.	
2017	Municipal Sewage Sludge	5.1	60.34	1.13	33.43	36.88	4.94	5.03	1.14	52.01	14.90	-	-	[38]
2017	SS from Waste Water Treatment Plant	7	50	3	40	27.9	4.7	4.5	1.4	34.6	12.50	28	3.5	[39]
2017	SS from Waste Water Treatment Plant	4.01	73.10	2.80	18.60	42.0	5.60	4.30	1.30	28.30	-	-	9.90	[40]
2016	SS from Waste Water Treatment Plant	5.6	54.2	8.6	37.2	40.6	7.1	7.7	3.3	41.2	11.1	-	-	[41]
2016	SS from Waste Water Treatment Plant	7.4	63.1	7.1	22.5	38.0	5.1	6.9	1.2	19.0	-	-		[42]

2016	SS from Waste Water Treatment Plant	5.8	54.1	6.0	34.2	34.9	4.8	4.5	1.1	14.8	-	-	-	[42]
2015	SS from Waste Water Treatment Plant	8.71	61.11	9.20	26.89	45.16	7.20	7.69	-	27.59	16.18	-	-	[43]
2015	SS from Waste Water Treatment Plant	1.67	52.22	1.84	46.11	28.94	4.48	4.23	0.65	13.92	13.04	-	-	[44]
2015	SS from Waste Water Treatment Plant	-	54.2	8.6	37.2	25.5	4.5	4.9	2.1	25.8	11.1	-	-	[45]
2014	SS from Waste Water Treatment Plant	4.43	68.57	16.42	15.01	53.24	7.39	6.12	-	33.25	24.2	-	-	[46]
2014	SS from Waste Water Treatment Plant	7.5	59.06	9.35	24.05	38.45	5.93	7.03	0.77	25.24	-	-	-	[47]
2014	SS from Waste Water Treatment Plant	7.18	38.05	4.77	50.0	24.53	3.19	4.8	0.15	10.4	10.4	-	-	[48]

2013	SS from Management Center	-	60.05	11.21	28.74	50.72	7.70	8.69	1.59	31.30	16.24	-	-	[49]
2013	SS from Municipal Waste Water Treatment Plant	-	73.7	0.40	25.9	37.9	5.5	6.20	-	50.4	-	-	-	[33]
2013	SS from Waste Water Treatment Plant	-	45.5	6.9	47.6	42.3	3.7	8.3	19.1	26.6	-	26	5.6	[50]

2.3 Thermal degradation characteristics of sewage sludge:

The performance of the thermal deprivation conducts for sewage sludge Investigated by inspecting pyrolysis conduct by assistance of thermogravimetric analysis. Thermogravimetric Analysis (TGA), a critical strategy in the direction of gauge the level of mass loss. For example, as for temperature and time and to analyze the warm disintegration conduct amid pyrolysis. It is additionally useful in concentrate the energy of debasement of natural material amid pyrolysis process [51][52]. Warm debasement is enter component in planning of maintainable pyrolysis and co-pyrolysis processes [53]. An audit of TGA and energy of corruption of substances amid pyrolysis can help in arranging and building up the modern pyrolysis [54].

DTG is a straightforward investigative instrument to discover the measure of mass misfortune or mass pick up of a solid as a component with temperature. It could assist to discover active constraints (actuation vitality, pre-exponential factor, request response) through various natural resources at isothermal and non-isothermal circumstances. Because of littler trial period and necessity of a lesser amount of trial information, procedure has vital significance. By looking at DTG bends, temperature by the side of which most extreme rate mass misfortune show up, can be dictated by the position of the crests [55]. The thermogravimetric investigation system necessitates insignificant amount of feedstocks, exact regulator and simple in work [56].

Table 2.2 spoke to the entire writing overview of thermal disintegration of sewage sludge through thermogravimetric analysis. By writing study as recorded underneath in Table 2.2 comprehensive pyrolysis conduct by utilizing TGA_DTA strategy can be partitioned into three fundamental stage. Second stage begins from 200-600°C speaks to the deterioration of biodegradable natural issue, examples are proteinases material, carboxylic acids and cellulose. Disintegration of non-biodegradable resources like aromatics, soaked aliphatic, and long chain aliphatic amides, nitriles. In preceding stage >600°C, decay of inanimate like calcium carbonate befall [57][58]. Hyuk et al. spoken about TGA_DTG examinations meant for essential pinnacle of sewage ooze acquired through squander water treatment plant shows up scope of 250– 500 °C face most extreme change temperature 274°C, cover pinnacle of wood and optional pinnacle got at nearly 500– 600 °C with greatest transformation temperature 345°C incompletely like the pinnacle of coal [59].

Table 2.2: Investigation on thermal behaviors of sewage sludge using TGA

Year	Sample	Heating rate °C/min	Temp. °C	Mass loss temperature ranges °C			T_i (°C)	Tf (°C)	T_{max} (°C)	DTG_{max} Wt %/min	Residue (wt%)	Ref.
				Stage 1	Stage 2	Stage 3						
2017	Sewage sludge	20	50-900	50-200	200-400	400-900	250, 450,	370, 570,	298, 345, 530	-	43	[60]
2017	Sewage sludge	20	25-900	25-200	200-500	500-600	200, 450	450, 500	274, 351, 385	-	25	[59]
2016	Sewage sludge	10	25-1000	25-200	200-600	600-1000	210	600	328	0.21	37.5	[61]
2016	Sewage sludge	10	25-1000	25-150	150-800	>800	240	584	250, 550	1.10	39.85	[62]
2016	Sewage sludge	5	25-1000	25-200	200-650	<650	227	627	563	0.34	-	[63]
2015	Sewage sludge	10	25-1000	<180	180-600	>600	210	550	328	0.21	37.5	[64]
2015	Municipal solid waste	30	35-900	35-150	180-550	>550	180	550	337	0.90	67.3	[65]
2015	Sewage sludge	10	30-900	20-180	180-550	>550	180	550	390	-	-	[66]
2014	Sewage sludge	10	25-900	25-150	150-450	450-600	300	450	340	0.65	-	[67]

2014	Sewage Sludge	10	30-800	<120	130-492	492-720	276	454	276, 333	-	44.23	[47]
2013	Sewage sludge	10	25-800	25-180	180-600	>600	180, 550	390, 800	283, 336	-	16.4	[68]
2012	Sewage sludge	20	25-800	25-200	200-500	>500	200	500	290, 350	0.30	-	[69]
2012	Sewage Sludge	20	25-1000	25-200	200-550	>650	170	550	350	-	-	[70]

2.4 Poly-generation and application of Pyrolysis:

Sewage sludge pyrolysis has authentic significance because of creation of bio solids and bio oil which is exceptionally valuable in energizes and power generation. It can also deliver the non-convertible gases for example H_2, CO, CO_2, CH_4, C_2H_2, C_2H_6, and different carbon based components in vapor form [71]. Pyrolysis contains thermal decay of various natural constituents without oxidative condition. Pyrolysis be situated into three fundamental unites moderate pyrolysis, quick pyrolysis and flash pyrolysis as indicated by their temperature ranges and diverse living arrangement time. Inferior temperature and lengthier living arrangement period generate bio-scorch. Greater temperature and reduced habitation time give greater number of vapors. Intermediate temperature and short living arrangement time bounces oil and termed as quick pyrolysis. Oil got from quick pyrolysis is least expensive source exclusively [72]. To enhance item eminence and progression effectiveness, diverse kinds of novel pyrolysis advances like partial pyrolysis, hydro-treating of pyrolysis, auto-warm pyrolysis, hydro pyrolysis, in situ and ex situ synergist pyrolysis are beneath creating circumstance to get distinctive strong, fluid and vaporous item. All these items create through entire sorts of pyrolysis with various proportions by fluctuating the functioning parameter [73][74].

Three unique reactors to be specific fixed bed, fluidized bed, and moving bed reactor utilized to direct the pyrolysis procedure. By and large, settled bed reactors can be utilized as a part of moderate and microwave pyrolysis and fluidized bed containers used to accomplish fast pyrolysis process [75]. Table 2.3 describe that the category and product nature of sewage sludge depends upon different operating constraints.

Table 2.3: Investigation on thermal behaviors of sewage sludge using TGA

Year	Type of Pyrolysis	Type of Reactor	Sample	Operating Conditions						Product	Ref.
				Weight of Sample	Temp.	Residence time	Heating Rates	Duration	Sweep flow rate		
2017	Fast pyrolysis	Fixed bed reactor	Sewage sludge	300g	400-450°C	-	10-200 °C/s	25min	-	Bio-oil	[76]
2017	Primary pyrolysis	Pyrolyzer with GC/MS	Sewage Sludge	1.3mg	300-900°C	2sec	20°C/ms	2-10min	1ml/min	Bio-char	[77]
2017	Continuous pyrolysis	Spiral screw reactor	Sewage Sludge	-	400-800°C	6-46min	-	-	-	Bio-oil	[78]
2017	Fast pyrolysis	Micro reactor system	Sewage sludge	0.5mg	400-800°C	-	-		90ml/min	Gas and bio char	[40]
2016	Fast pyrolysis	Electric furnace	Sewage sludge	24g	100-800°C	08min	-	8min	10l/min	Bio-oil	[79]
2016	Fast pyrolysis	conical spouted bed reactor	Sewage sludge	50g	450-600°C	10min	-	50min	14Nl/min	Bio oil	[41]
2016	Slow pyrolysis	Batch reactor	Sewage sludge	-	200-850°C	Few seconds	10°C/min	-	1l/min	Bio char	[80]

2016	Fast pyrolysis	Curie-point pyrolyzer	Sewage sludge	1mg	300-700°C	5sec	-	20min	3ml/min	Bio-oil	[81]
2015	Flash pyrolysis	Conical spouted bed reactor	Sewage Sludge	50g	450-600°C	>1sec	-	50min	30l/min	Volatile gases	[44]
2015	Slow pyrolysis	Fixed bed reactor	Sewage Sludge	5g	400-600°C	-	20°C/min	40min	20ml/min	Bio char	[82]
2015	Fast pyrolysis	Fixed bed reactor	Sewage Sludge	35g	400-600°C	-	-	50min	500ml/min	Char and bio oil	[83]
2014	Slow pyrolysis	Fixed-bed Reactor	Sewage Sludge	2g	300-700°C	2.7sec	10°C/min	60min	300ml/min	Bio char	[84]
2014	Fast pyrolysis	Microwave oven	Sewage sludge	15g	450-600°C	-	5°C/min	-	1.2ml/min	Bio oil	[85]

2.5 Kinetic Models:

This part quickly depict the regular thermal conversion kinetic models which have been successfully connected for sewage muck. Normally sewage slime pyrolysis contains immense number of concoction responses, intermediates and items that are produced amid entire process. Pyrolysis actuation vitality Ea and pre-exponential factor A can be roughly decided by TGA information in modest kinetic model approach. Intended for reason, information regarding response component isn't obligatory. These kind of scheming are called "kinetic free model" and these kinetic free models give exceptionally constrained kinetic informations, activation energy and pre-exponential factor.

Then again, more comprehensive kinetic methodologies anticipate solid char and volatiles are pyrolysis results by sewage muck transformation, measure of outcomes isn't relevant [86]. As indicated by this idea, one or various response models are created, in which components of sewage ooze can be specifically changed over to their separate items in just a single stage. Other dynamic model tactic in which sewage slime is initially changed over unstable element and beginning items in the essential response and after that the unstable product changed over into desired substance. This kinetic model approch is called two-step or consecutive-reaction model. Volatiles items in these models approch comprises of both convertable and non-convertible gases at elevated temperatures. In these models unstable gases incorporates in light of the fact that condensable gases can be additionally changed over into fluid items.

Table 2.4: TGA pyrolysis for kinetic studies for sewage sludge

Sample	**Initial mass (mg)**	**Temp. Range (C)**	**Heating Rate (°C/min)**	**Inert Gas Flow Rate (ml/min)**	**Kinetic Model**	**Activation Energy E (KJ/mol)**	**Ref.**
Sewage sludge	5	25-900	20	20	First order reaction models	296.8±0.5 346.5±0.6 385.0±3.5 521.7±0.4	[59]
Sewage sludge	5-25	25-900	20	30	Friedman method	525.16	[61]
Sewage sludge	10	25-1000	10	80	KAS method, Starink method	253.6 253.3	[63]
Sewage sludge	10	25-1000	5	80	Distributed activated energy model	34.32-140.02 70.36-150.91	[62]
Sewage sludge	10	25-900	5-25	40	Midilli Method, non –isotherm models	18.03-11.87 33.61-47.37 20.47-33.43	[87]
Municipal solid waste	20	30-900	10,30,50	30	Distributed activated energy model	150-840	[65]
Sewage sludge	5-25	30-900	10	20	Distributed activated energy model	48.84, 37.7	[66]

Sewage Sludge	10-20	30-800	10	30	Arhenius law, coats and redferm model	82.28, 48.34	[78]
Sewage Sludge	-	25-700	5-30	40	Ozawa method, Satava method	137.9-157.2 128.4,164.7, 212.02	[88]
Sewage sludge	12	25-800	10	50	Arhenius kinetic model	197.7, 169.6	[68]
Sewage sludge	-	25-800	20	30	Coats Redfern method	5.75 4.42 4.41	[69]
Sewage Sludge	-	25-1000	20	10	Consective reaction model, Simha and wall Model	119.86 100.09 258.31	[70]
Sewage sludge	6	100-1000	20	20	FR, KAS, FWO, Vyazovkin methods	137.87 80.180 155.17	[89]
Sewage Sludge	10	25-1100	10	100	Coats Redfern Method	23.3	[90]
Seawage sludge	10	150-700	10	10	Arrhenius kinetic model	79.07 191.42 80.72 200.67 101.14	[91]

Chapter 3

Material and Methodology

3.1 Raw Material:

The sewage sludge was attained through MBR domestic wastewater treatment plant located in NUST Islamabad. Obtained sample was primarily air desiccated for a week to remove the surface moisture, then the sample was dried in an electric oven for a day at 105±5°C until the constant weight was obtained to remove the inbound moisture contents. Drying is an essential part before the start of characterization because it can highly effect the calorific value. The sewage sludge sample was crushed with mortar and pestle. Then sample was ground into fine powder which was sieved through 1000µm screen and stored into air tight bags before further analysis.

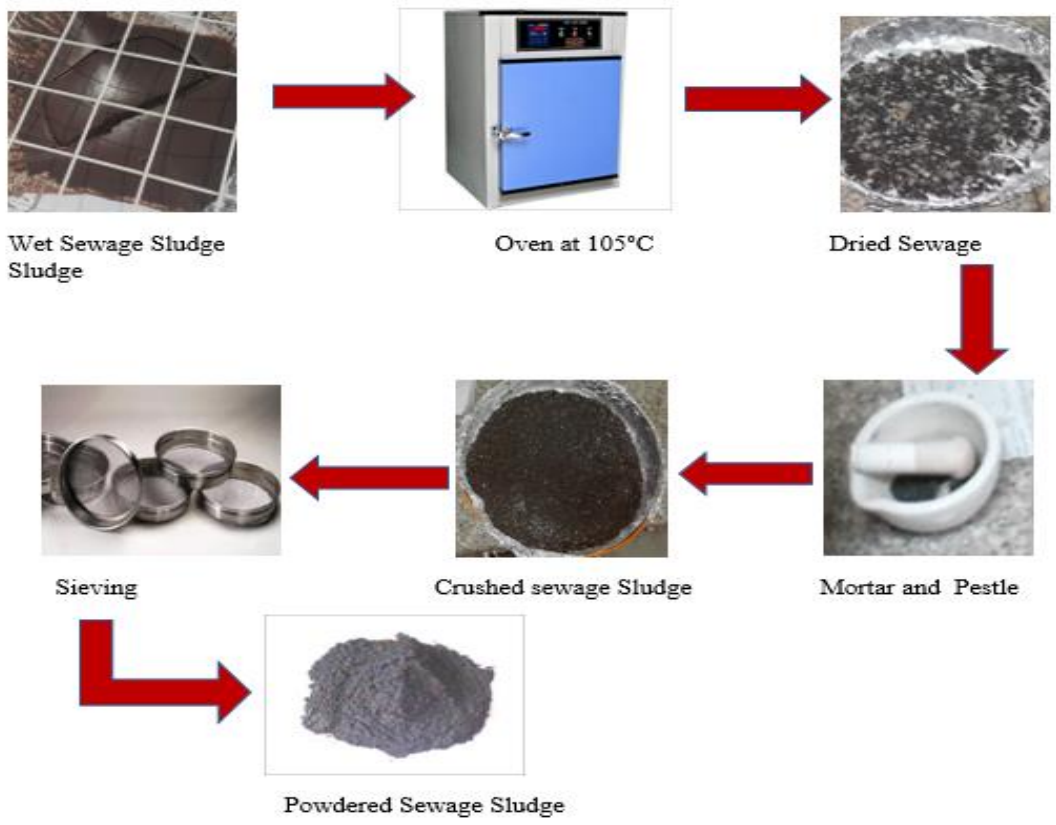

Figure 2.1: Drying and size reduction of sewage sludge

3.2 Characterization of Sewage Sludge:

3.2.1 Proximate Analysis of Sewage Sludge:

Proximate analysis was performed in electric oven and muffle furnace according to ASTM Standards method to determine the percentage of M, VM, FC and ash. For weight percentage of different contents, initially 5g of sewage sludge is used to burn at specific conditions until the weight became constant according to ASTM D4442 standard method [92]. The percentage of different elements was calculated by using the following equation.

$$\text{Percentage of element} = \frac{m_i - m_f}{m_i} \times 100 \qquad 3.1$$

m_i is initial weight placed in oven and m_f is weight after drying of sewage sludge at 110°C in electric oven. Table 3.1 represents the specific condition and equipment used to calculate the percentage of M, VM, ash and FC [92][93].

Table 3.1: Specific condition and equipment used in proximate analysis

Components	**Instrument**	**Temperature and Time**
Moisture (M) removal	Electric oven	110℃ for 24 hrs.
Volatile matters (VM)	Muffle furnace	700℃ for 7min
Ash sample	Muffle furnace	900℃ for 3 hrs
Fixed carbon (FC)	= (100 - (M%+VM%+ASH%))	

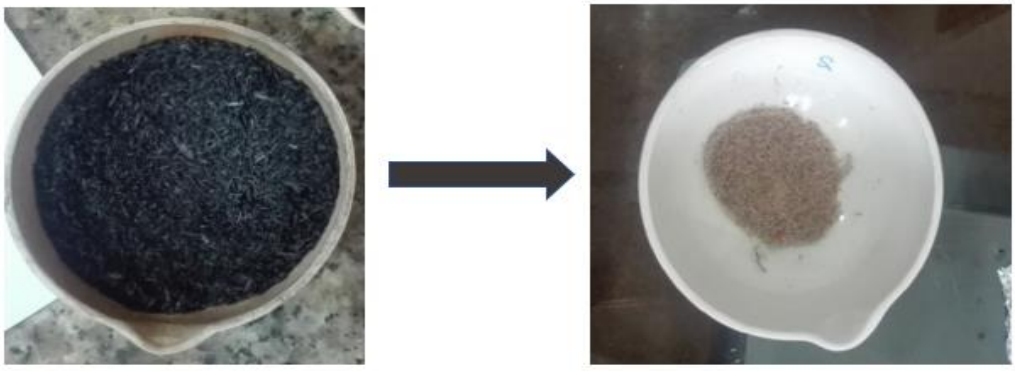

Initial form of sewage sludge Final form of sewage sludge after burning

Figure 3.2: Initial and final form of sewage sludge after proximate analysis

3.2.2 Ultimate Analysis of Sewage Sludge:

Ultimate analysis was achieved through CHNS elementary analyzer (PerkinElmer 2400II, USA) to obtain the percentage of C, N, H, N and O. Bomb calorimeter was used to determine high calorific value according to given ASTM standards[94].

The High Heating Value (HHV) designates the amount of energy to be progressed from the sewage sludge sample. Salam et al. told in his study that the tentative measures to determine the HHV contain significant flaws so numerous correlation model equations were established to measure the HHV [95].

Figure 3.3: CHNS elemental analyzer (PerkinElmer 2400II, USA)

3.2.3 FTIR of Sewage Sludge:

Chemical functional group present in the sewage sludge sample was examined by means of PerkinElmer spectrum 100 FT-IR Spectrometer. Sample was used by making pellets with KBr in 1:100 ratio. The resolution was kept at $4cm^{-1}$. The IR scanning range was 400 to $4000cm^{-1}$. Fourier transform is termed for this type of spectroscopy because the spectra obtained through this spectroscopy is based on Fourier transform mathematical process. This is used to achieve the qualitative and quantitative analysis of material

In FTIR technique IR radiations intermingle with the sewage sludge pellet with kBr. Some radiations are captivated by the sewage sludge sample and some are transmitted through sewage sludge. Based on absorbed and transmitted radiations, attained spectrum is known as FTIR spectrum. The subsequent spectrum generates a finger print of the sludge sample, used to identify the functional group.

The covalent bonds are elastic and always in a state of a vibration. Vibration could be bending or stretching. The vibrational motion influenced by these molecules is the appearances of their particular atoms. All organic compounds are capable of absorbing IR which matches to their vibration. IR spectrum obtained is a graph between percentage transmittance and wavenumber in cm^{-1}[96].

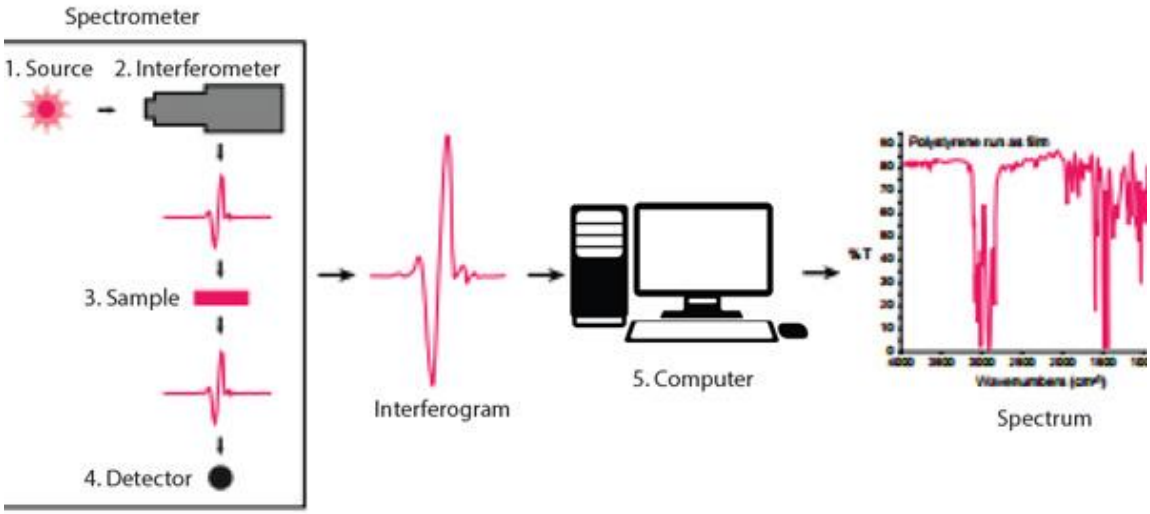

Figure 3.4 : Working principal of Fourier transform infrared spectroscopy [96].

3.3 Thermal Degradation Behavior of sewage sludge through TGA:

The thermal degradation behavior of sewage sludge pyrolysis was determined by using thermogravimetric analyzer under nitrogen environment. Flow of nitrogen was kept as 200ml/min with temperature range of 25-800°C. Initial mass of sewage sludge sample was 10±3mg. Heating rate was 5, 10 and 20°C/min at which the mass loss and rate of mass ploss was determined with respect to temperature and time. The slow heating rate was chosen to overlook the heat transfer restrictions. To achieve the maximum accuracy and least error experiment was repeat at least three times. Data obtained from TGA and DTA both helped to understand the thermal decomposition behavior during pyrolysis process and also in estimation of kinetics and thermodynamic parameters of sewage sludge pyrolysis.

Thermogravimetric analyzer consists of a pan positioned in a programmable incinerator. This pan is braced by a delicate precision balance. The sludge is placed onto the pan with a predefined heating rate and a temperature range at which changes is in sample is to be detected is given to the incinerator. The incinerator is heated from a lower temperature and reaches the maximum temperature and then it is cooled. The mass loss is observed during the entire process. The atmosphere of the incinerator is controlled by an inert gas such as nitrogen or helium. The data obtained from TG analysis of the sewage sludge permits the interpretation of loss of volatile components in sludge, its thermal steadiness, and disintegration. The data attained is graphed among temperature range on x-axis and percentage mass loss on y-axis [97].

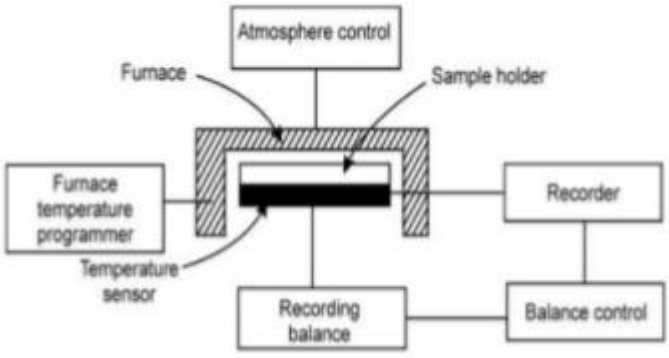

Figure 3.5: Working principal of TGA [97]

3.4 Kinetic Analysis:

3.4.1 Fundamental Kinetic Expressions:

The kinetic analysis of sewage sludge pyrolysis was simply determined by Arrhenius law which provided information about rate of reaction occur during pyrolysis reaction. The basic equation used for kinetic analysis of pyrolysis of sewage sludge was given below

$$\frac{d\alpha}{dt} = k(T)f(\alpha) \qquad 3.2$$

Where

$$\alpha = \frac{m_i - m}{m_i - m_f} \qquad 3.3$$

In which m_i is initial mass, m is mass at given time t and m_f is final mass in mg.

$$k(T) = A\exp\left(-\frac{Ea}{RT}\right) \qquad 3.4$$

In which A is pre-exponential factor (min^{-1}), Ea is activation energy (KJ/mole), R is universal gas constant (0.008314kJ/moleK) and T is absolute temperature.

And

$$f(\alpha) = (1-\alpha)^n \qquad 3.5$$

In which n is reaction order. For constant heating rates $\beta = \frac{dt}{dT}$ So equation 3.2, 3.3 and 3.4 can be written in combined form.

$$\frac{d\alpha}{dT} = A\exp(-\frac{Ea}{RT})(1-\alpha)^n \qquad 3.6$$

By applying integration to equation 3.6, a new equation is obtained

$$g(\alpha) = \int_0^{\alpha} \frac{d\alpha}{f(\alpha)} = \frac{A}{\beta}\int_{T0}^{T} \exp(-\frac{Ea}{RT})dT \qquad 3.7$$

Where g(α) is integral form of reaction model. To find out the analytical solution of right side of equation is impossible so various approximation models are used to solve the complicated part of this equation.

3.4.2 Model Fitting Approach:

3.4.2.1 The Coats and Redfern Model:

Coats and Redfern method is extensively used to estimate the pre-exponential factor and activation energy to predict the order of reaction. Basic equation for coats and Redfern method is given below

$$\ln\left(\frac{g(\alpha)}{T^2}\right) = ln\frac{AR}{\beta Ea}\left(1-\frac{2RT}{Ea}\right)-\frac{Ea}{RT} \qquad 3.8$$

Where β is heating rate, R is universal constant (0.008314 kJ/mole K) ang g(α) is kinetic function of different reaction mechanisms and developed model obtained from integration of f(α). Therefore, activation energy can be obtained by drawing a graph between 1/T and ln(g(α)/T²) and by obtaining slope from drawn straight line. Pre-exponential factor can be obtained from intercept of this graph. g(a) can be varied according to different developed model and reaction mechanisms. Some of which is listed below in Table 3.2 [98][99]

Table 3.2: Kinetic model name with their respective g(a)

MODEL NAME	**g(α)**
Chemical Reaction Order 1	-ln(1-α)
Chemical Reaction Order 1.5	$6(1-\alpha)^{-1/2}$
Parabolic law 1D	α^2
Va lensi equation 2D	$\alpha + (1-\alpha)\ln(1-\alpha)$
Ginstling-Broushtein equation 3D	$(1-2/3\alpha)-(1-\alpha)^{2/3}$
Avrami-Erofeev equation Nucleation and growth (n = 1.5)	$[-\ln(1-\alpha)]^{2/3}$
Avrami-Erofeev equation Nucleation and growth (n = 2)	$[-\ln(1-\alpha)]^{1/2}$
Phase interfacial reaction Shrinkage geometrical (column)	$1-(1-\alpha)^{1/2}$

Phase interfacial reaction Shrinkage geometrical (Spherical)	$1 – (1 – \alpha)^{1/3}$
Power law	(α)

3.4.3 Model Free Approach

3.4.3.1 Flynn-Wall-Ozawa Method (FWO):

This model is used to calculate activation energy based on degree of conversion. Calculated values fluctuates with conversion as the reaction progress. This model is frequently used for estimation of merged dense proellent and is appropriate for inquiry of diverse resources. The simplest form of Flynn-Wall-Ozawa method is given below:

$$ln\beta = \ln\left(\frac{AE}{Rg(\alpha)}\right) - 5.523 - 1.0518\left(\frac{E}{RT}\right) \qquad 3.10$$

kinetic graph is strategized beteen 1/T and lnβ for various degree of conversion. The slope and intercept is used to calculate E and A.

3.4.3.2 Friedman Method:

It is renowned model among investigators in the arena of energatic ingredients. It is type of model free approch. The final form of Friedman model is given below:

$$\ln\left(\beta\frac{d(\alpha)}{dT}\right) = \ln[Af(\alpha)] - \frac{E}{RT} \qquad 3.11$$

Kinetic constraints canbe premeditated by drawing a graph between $\ln\left(\beta\frac{d\alpha}{dt}\right)$ versus 1/T at different heating rates at different degree of conversion

3.4.3.3 Kissinger-Akahira-Sunose Method:

The KAS model is alike original Kassinger method. Only difference is in temperatures used in kinentic designs. KAS model uses the sample temperature corresponds to each degree of conversion (Tα) instad of peak temperature (Tp). This method can be explained by the equation given below

$$\ln\left(\frac{\beta}{T\alpha^2}\right) = \ln\left(\frac{A.R}{Eag(\alpha)}\right) - \frac{Ea}{RT\alpha} \qquad 3.12$$

. Activation energy and exponential factor attained by drawing a plot for value of temperature and function derived by simple equation from arrhenius law and conversion rate by calculating slope and intercept[100][101].

3.4.3.4 Popescu Method:

However, as E_a varies with α OFW and KAS creates systematic errors, which can be avoided using integral segments of $\Delta\alpha$ as in the case of Popescu method.

$$\ln\left(\frac{\beta}{T_\alpha - T_{\alpha-\Delta\alpha}}\right) = const - \frac{2E_a}{R(T_\alpha + T_{\alpha-\Delta\alpha})} \qquad 3.13$$

where $\Delta\alpha$ is the conversion interval, $T_{\alpha-\Delta\alpha}$ is the absolute temperature at $\alpha - \Delta\alpha$ and T_α is the temperature corresponding to α. The relative integration errors in Popescu method can be further reduced by making $\Delta\alpha$ interval smaller.

3.5 Thermodynamic Analysis:

Kim et al. established a relationship which provides information about thermodynamic parameters[102]. Thermodynamic parameters which can be taken into consideration was change in enthalpy, Gibbs free energy and entropy. These parameters can be calculated based on kinetic data of sewage sludge pyrolysis. Following equations are used to determine kinetic

$$\Delta H = Ea - RT \qquad 3.14$$

$$\Delta G = Ea + RT_m ln\left(\frac{K_B T}{hA}\right) \qquad 3.15$$

Where K_B is Boltzmann constant which is equal to $1.381*10^{-23}$ m^2 kg/s^{-2} K^{-1}. T_m is maximum temperature at which maximum decomposition occur. h is planks constant which is equal $6.626*10^{-34}$ m^2kg/s and R is universal gas constant equal to 0.008314Kj/Kmole.

$$\Delta S = \frac{\Delta H - \Delta G}{T} \qquad 3.16$$

3.6 Thermal Degradation Behavior through Autoclave Pyrolyzer Unit:

The pyrolysis tests of dried sewage sludge samples were achieved in single mode autoclave pyrolyzer unit at various temperature 350°C, 400°C and 450°C by keeping all other condition like pressure, agitation speed and amount of sample constant for each run. The autoclave pyrolyzer unit is consist of SS 360L vessel made up of stainless steel material with $1dm^3$ capacity. In an individual run, amount of 150g of sewage sludge sample is kept into the vessel (20.32cm length × 10.16cm I.D) which is air tight. A continues agitation is applied throughout the process at 25.6Hz speed. Inert atmosphere is created by suction applied through pump with negative pressure of 50kPa. A schematic diagram of the experimental setup is shown in Figure 3.6.1.

The system is heated at a rate of 10°C/min to the required temperature, and sustained there for half an hour time to provide it enough time for thermal degradation. After completing this time duration at fixed temperature, the release of pyrolysis products from the autoclave pyrolyzer unit is being ended. Throughout the run, the vapors produced in the vessel evolved from upper side of vessel and entered into condenser where the liquids are condensed and collected. The uncondensed gases were normally expelled either in atmosphere or in gas bags for the analysis and characterization of pyrolysis gases. Burned solid product can be calculated from the bottom of autoclave vessel. The yield of solid char, pyrolysis liquid and gases were determined in each experiment by weighing the amount of sample used in each run and amount of product obtained by using following formula.

$$yield\ \% = \frac{amount\ of\ sample}{amount\ of\ product} \times 100 \qquad 3.17$$

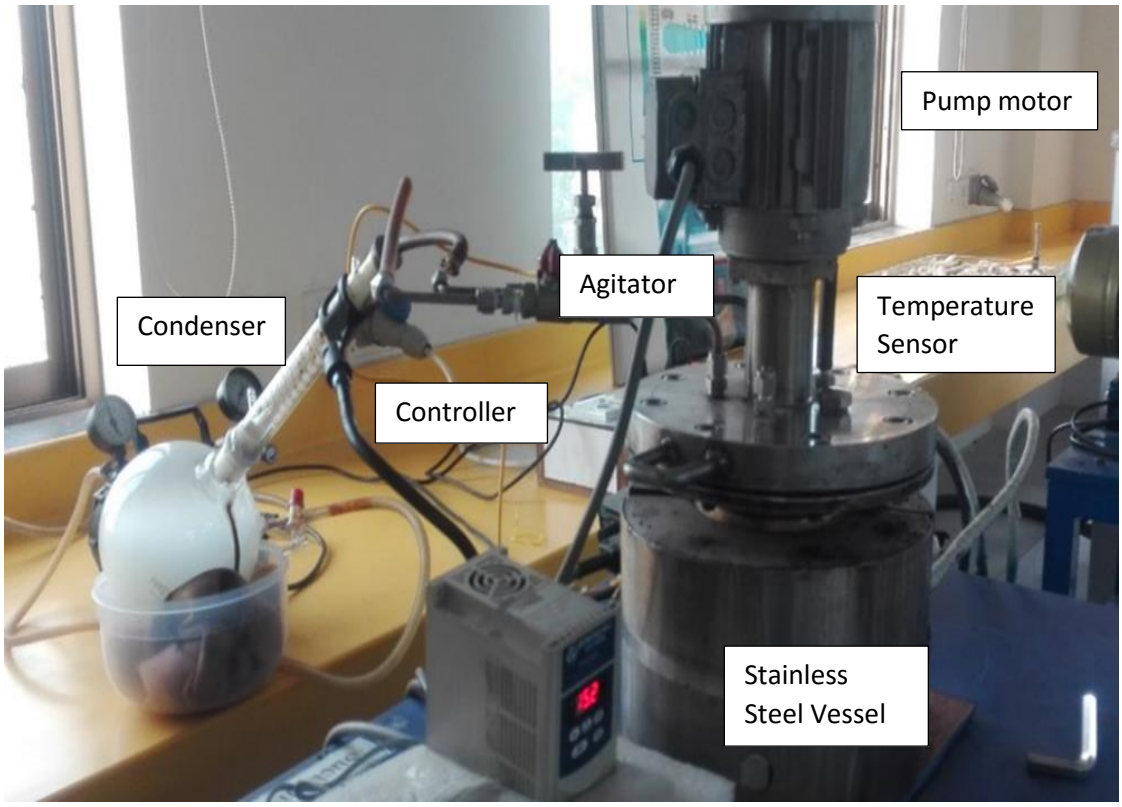

Figure 3.6: Original diagram of autoclave pyrolyzer unit

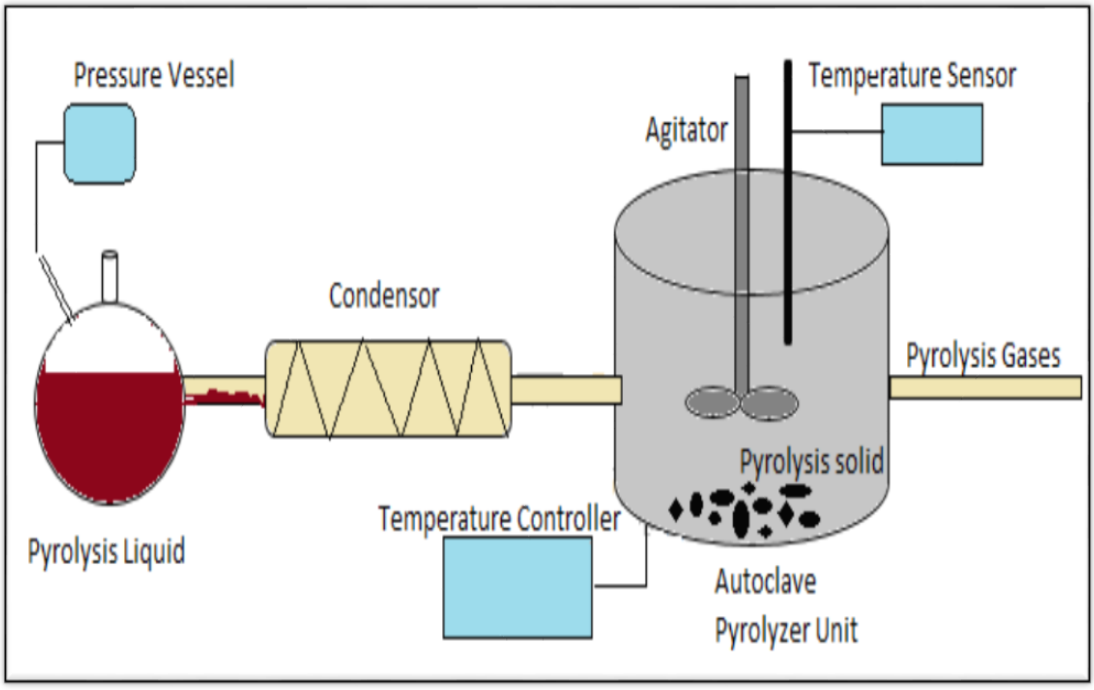

Figure 3.7: Block diagram of autoclave pyrolyzer unit

3.7 Characterization of pyrolysis Products:

3.7.1 Gas chromatography–mass spectrometry (GC–MS) of Liquid Oil:

The liquid oil attained from pyrolysis of sewage sludge dissolved in chloroform and analyzed through GC-MS using a SHIMADZU QP 2020 gas chromatograph coupled to an HP 5973 quadrupole detector. The gas chromatograph was attached with a 30m × 0.25 mm capillary column layered with a 0.25 µm dense film of 5% phenyl methyl poly-siloxane. Helium (He) was used as a carrier gas at a consistent flow of 0.9 mL/min. Initially, the temperature was 40°C kept for 5min and then settled from 40°C to 300°C at the rate of 5°C/min with an isothermal kept for 30min. Entire injection was passed out at 300°C and the purge valve was swapped on after 1min. The ion source temperature was 230°C and the transfer line temperature was 325°C. Data were assimilated in the full-scan mode between m/z 33–533 and 6min of solvent delay was used.

The components present in liquids were recognized by associating their mass spectra with standard spectra from the NIST mass spectral data library, considering the experimental fragmentation and assessing the retention times by comparing with standard components. Due to the presence of numerous components and functionalities in the elements investigated, calibration was not performed.

Figure 3.8: GC-MS SHIMADZU QP 2020 with HP 5973 quadrupole detector

3.7.2 Infrared spectroscopy (FTIR) of Char:

The solid product obtained from pyrolysis of sewage sludge is further analyzed by Infrared Spectroscopy (FTIR) which provided the information about functional group present in the material. The FTIR spectrum of solid char produced at temperature 350°C, 400°C and 450°C were collected by using PerkinElmer Spectrum 100 FT-IR Spectrometer with the resolution of $4cm^{-1}$. The pellets were prepared by using sample with KBr in ratio of 1:100. The range of wavenumber was selected from $400cm^{-1}$ to $4000cm^{-1}$ for all three solid char samples.

3.7.3 Thermogravimetric Analysis (TGA) of Char:

To study the thermal degradation behavior, thermogravimetric Analysis of solid product obtained from sewage sludge pyrolysis at various temperature 350°C, 400°C and 450°C is carried out in SHIMADZU DTG-60 DTG-60H thermogravimetric analyzer. In each experiment, the small amount of sample about 8±2mg is placed in sample holder and nitrogen N2 is provided with flow rate of 200ml/min to create inert atmosphere. The experiment is carried out in the temperature range of 35°C to 800°C with heating rate of 20°C/min.

3.7.4 Gas Chromatography with TCD detector of Gaseous Product:

The non-convertible gases obtained from autoclave pyrolyzer unit were collected in a gas bags from nozzle at the end of the condenser so that gases could be collected without encountering environmental air. These gaseous samples obtained at 350°C, 400°C and 450°C were analyzed in an SHIMADZU GC-2010 Plus gas chromatograph attached with a TCD detector. An RT Molecular Sieve 5A, with ID 15224 having 30m length and 0.32mm ID. The column film thickness was 30µm with maximum temperature at 300°C. The oven temperature was initially at 35°C and equilibrium time was 3min. The helium was carrier gas with flow rate of 20mL/min. The injector temperature was 80°C and detector temperature was 220°C. The TCD was standardized with a typical gas mixture after specific period.

Figure 3.9: SHIMADZU GC-2010 plus gas chromatograph with TCD detector

Chapter 4

Result and Discussion

4.1 Characterization of Sewage Sludge:

4.1.1 Proximate Analysis of Sewage Sludge

Figure 4.1 depicts the proximate analysis of sewage sludge sample which illustrates the organic matter content of sample. The sewage sludge sample contained higher percentage of volatile matters 44.6% and ash 44.6% on dry basis but it has lower percentage of moisture 6.5% and fixed carbon 4.3% on dry basis. These proportions of volatiles in sample favors for thermal degradation processes because desirable products could be obtained by utilizing such material. Lower percentage of moisture content <10% provided higher yield of biofuels. Ash contain a certain amount of Fe, Ca, Mg and K which can be used activated catalyst for the pyrolysis reaction[103].

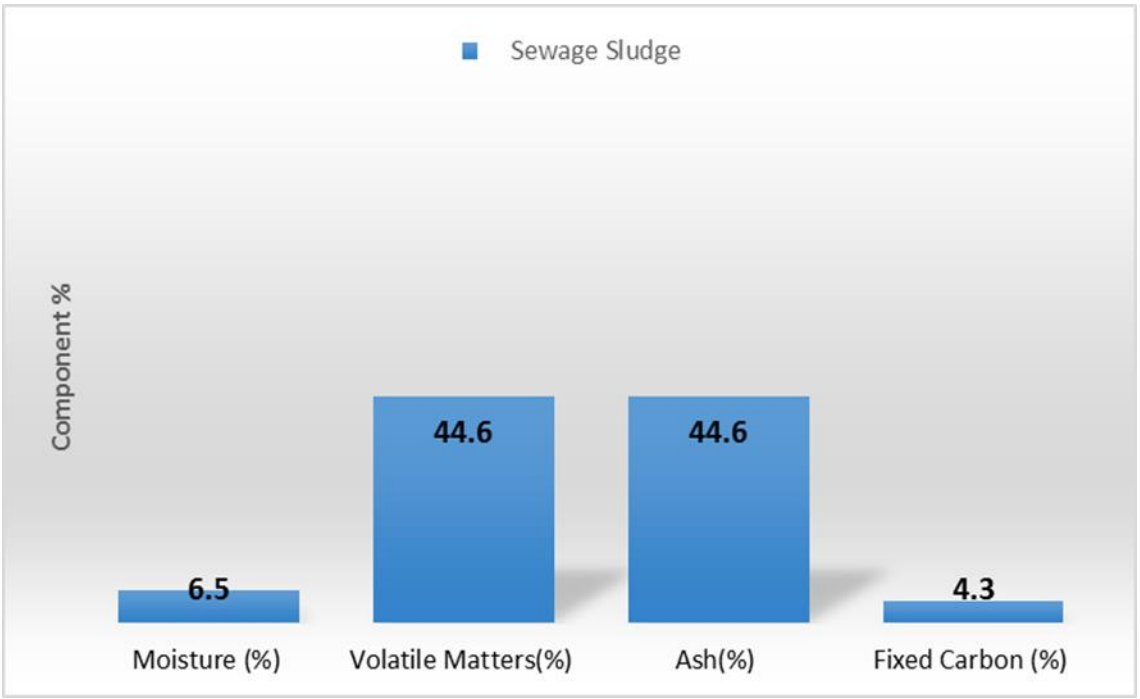

Figure 4.1: Percentage components of sewage sludge through proximate analysis

4.1.2 Ultimate Analysis of Sewage Sludge:

Figure 4.2 depicts the ultimate analysis of sewage sludge sample which illustrated the chemical composition of sample. The sewage sludge sample has higher percentage of oxygen contents (O) 45.7% and carbon content (C) 40.4% on dry basis but it contained lower percentage of hydrogen (H) and nitrogen (N), 6.2% and 6.7%, respectively. It also has very slight percentage of sulfur 1%. Xinyang et al. performed ultimate and proximate analysis of municipal sludge and indicated the larger fraction of volatile matters 60.34%, ash 33.43%, carbon 36.88% and oxygen 52.01% and lower percentage of moisture 5.1%, fixed carbon 1.13%, hydrogen 4.94% and nitrogen 5.03% [104].

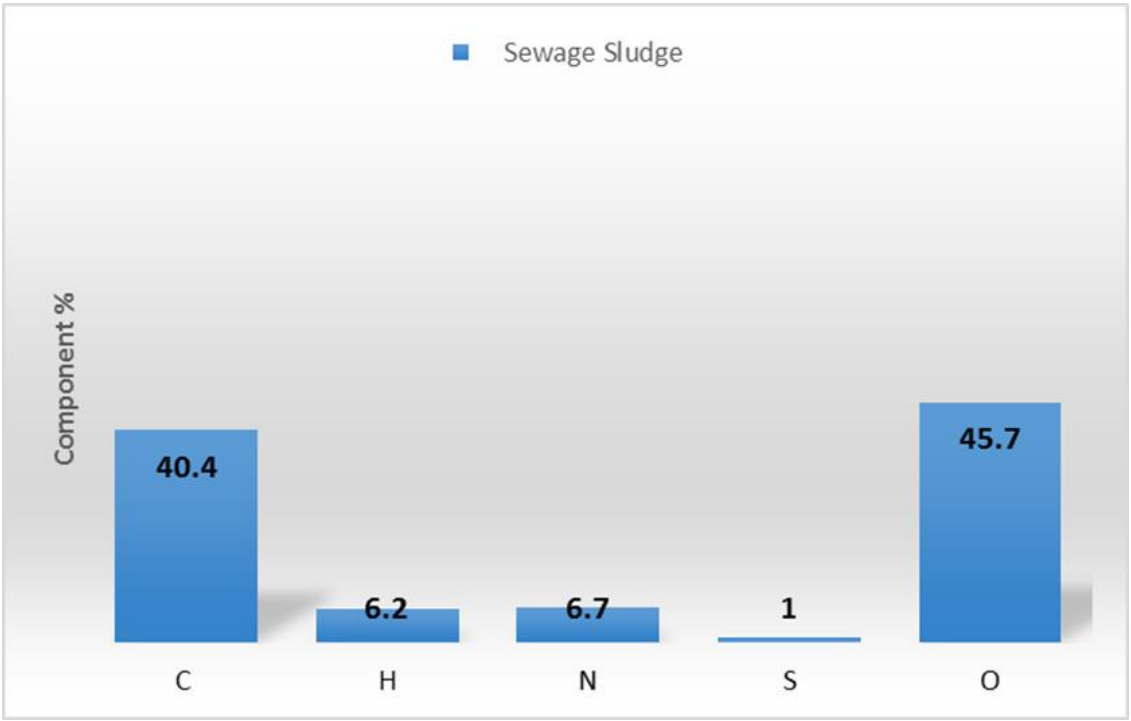

Figure 4.2: Percentage Component of sewage sludge through ultimate analysis

The calculated high heating value of sewage sludge sample was 19.5MJ/kg. The higher heating value of sewage sludge sample primarily depends upon the percentage of moisture present in it. When sample contains lower moisture content is, heating values becomes greater. The moisture free sewage sludge sample usually contain higher heating range from 5-20 MJ/kg [105]. Jing-pei Cao et al. and Wu Zuo et al calculated higher heating value of sewage sludge obtained from waste water treatment plant with

the help of bomb calorimeter and diverse types of formulas and developed correlations which was 16.24 and 10.4 MJ/kg[106].

4.1.3 Fourier Transform Infrared Spectroscopy (FTIR):

To comprehend the connection between the pyrolysis performance and chemical structure of sewage sludge sample obtained from municipal waste water treatment plant, the disseminations of numerous functional groups and types of bonds (single, double or triple) were perceived by FTIR analysis. FTIR spectra of sewage sludge sample was shown in Figure 4.3

The spectrum for sewage sludge sample exhibited a very broad and strong transmittance peak at 3444.92 cm-^{1} which identified the presence of O-H stretching vibration because in the range of 3650-3200cm^{-1} O-H or N-H stretching occur[107] Next assigned peak was at 2950cm^{-1} which identified the C-H regular and irregular Stretching vibration due to presence of aliphatic compounds. The range from 3300-2700cm^{-1} is specific for C-H stretching.

There were also two noticeable absorption peaks at 1634.37 and 1050cm-^{1}, that were appeared C=O and C-O function group stretching vibrations, respectively because range from 1780 to 1650 cm^{-1} is specified for C=O group and range from 1250-1000 cm^{-1} is specified for C-O group. The C=O group identified the presence of acids and aldehydes. Ma et al. and Zhao et al. detected absorption band at 1549 cm^{-1}, 1656cm^{-1} and 3420 cm^{-1} for primary and secondary amide group and O-H functional group, which provided the evidence of the presence of certain amount of protein in sludge sample [108].

In the range of 670–860 cm^{-1}, the absorption peaks are categorized by aromatic rings bending vibrations and the absorption peak at 1549, 1410 are for aromatic ring stretching vibrations. The range of 470–640 cm^{-1} is assigned for bending vibration of oxygen containing functional group with nitrogen, sulfur and phosphorus, respectively[109].

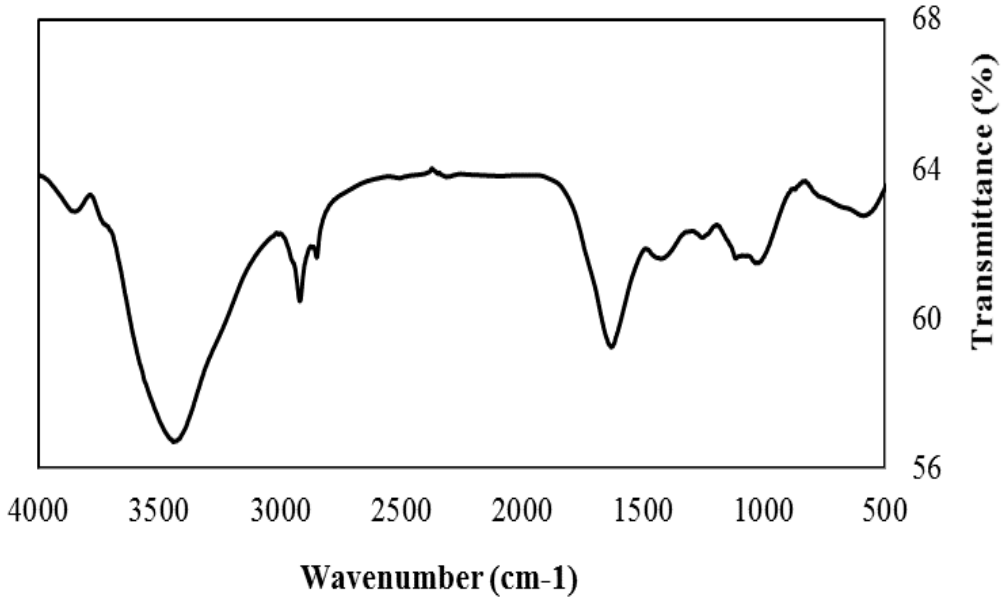

Figure 4.3: FTIR of sewage sludge sample obtained from municipal waste water treatment plant

4.2 Thermal degradation Behavior of Sewage Sludge through TGA:

4.2.1 TGA of Sewage Sludge:

Figure 4.4 represented three mass loss curves with respect to temperature at three different heating rates 5, 10 and 20°C/min. These three curves were mainly divided into three stages. Stage one involved removal of inbound moisture at 25-200°C. Second stage involved the disintegration of decomposable organic matter for example proteinases, carboxylic acids, cellulosic compounds) and the breakdown of non-convertible `carbon-based substance like aromatics, saturated aliphatic, and long chain aliphatic amides, nitriles at 200-600°C. Second range was the focal part of thermal degradation of sewage sludge because main disintegration occurs in this range. So, this range was further alienated into two ranges one is 200-400°C and other is 400-600°C. Third range was involved the disintegration of inorganic matters like calcium carbonate at above 600°C. Lopez et al. explained the TGA curve of sewage sludge sample and told that thermal degradation of biomass or other waste materials occur at 700°C and 400°C was minimum temperature at which substantial pyrolysis of sewage sludge sample took place [110].

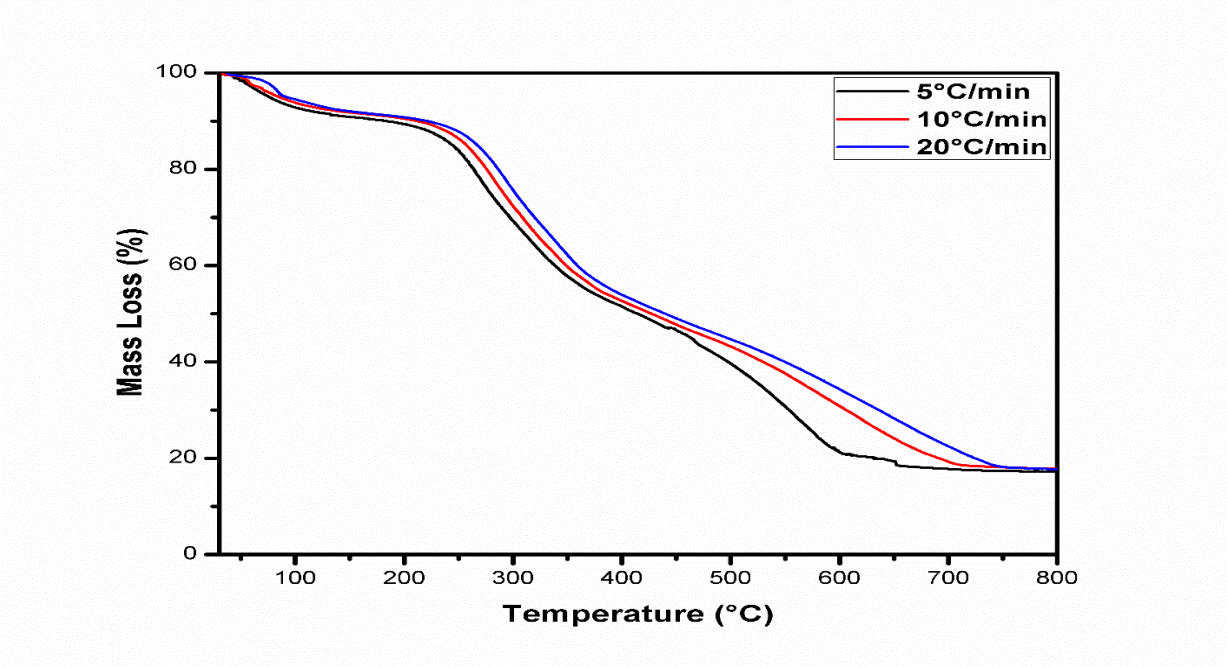

Figure 4.4: TGA of sewage sludge sample at 5, 10 and 20 ^{o}C/min

4.2.2 DTA of Sewage Sludge:

Figure 4.5 showed the DTA curves at 5, 10 and 20°C/min which provided characteristic temperature and percentage mass loss. It provides data about the heat loss or gain during decomposition process and indicated about reaction endothermicity or exothermicity. It also guesses the temperature at which the maximum mass loss occurs. It also gives information about percentage mass loss as each stage[111][112]. As mentioned above the main thermal degradation range was from 200°C to 600°C which was further separated into two ranges. In first range, maximum peak temperature T_m appeared at 285°C for 5 and 10°C/min with 55 and 65% mass loss and 310°C for 20°C/min with 75% mass loss at initial temperature (T_i)240°C to final temperature (T_f)330°. In second range, maximum peak temperature T_m appeared at 470°C for 5 and 10°C/min with 45 and 55% mass loss and 420°C with 65% mass loss at initial temperature (T_i) 400°C to final temperature (T_f) 550°C. The intensification of heating rate subsidizes to the slowing down of thermal degradation processes towards elevated temperatures, this fact could be enlightened that a high heating rate of sewage sludge sample with respect to given temperature in a short time as a result of increased thermal delay[108][109]. Secondly, the amount of released volatile matter reduced to some extent with increasing heating rate. On the other hand, the reduction in heating rates only relocated the peak temperature to lesser value without varying

thermal profile of disintegration, which could be due to the growth in heat fluctuating proficiency at lesser heating rates compared to advanced heating rates.

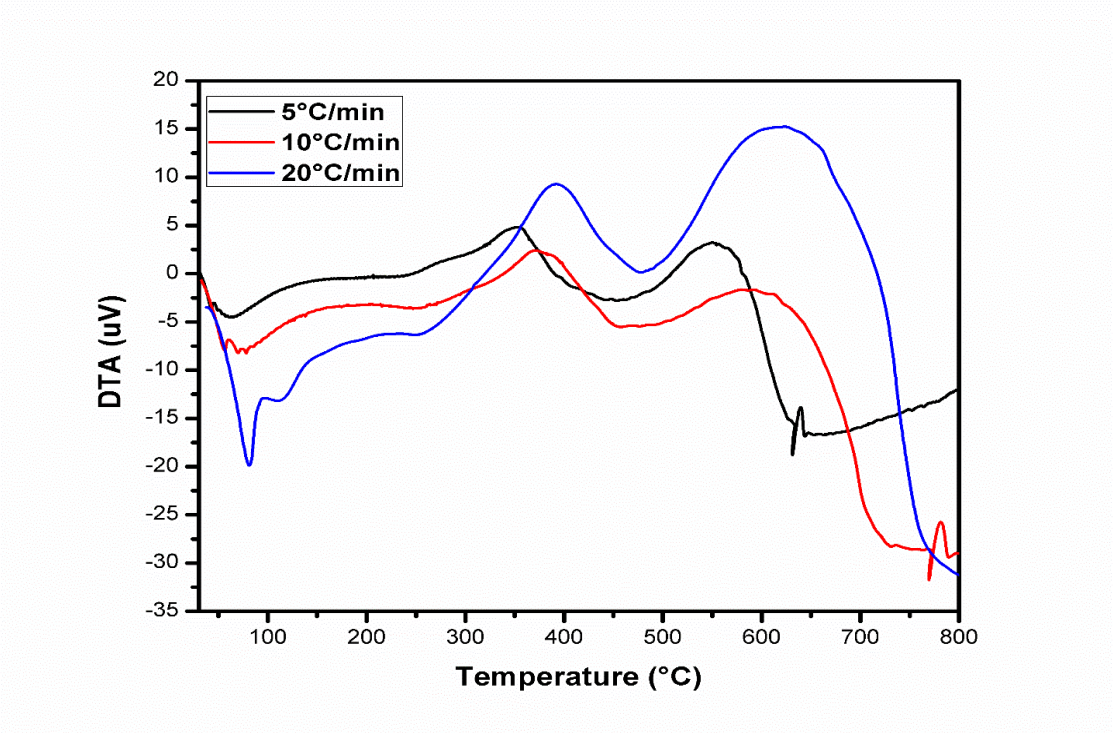

Figure 4.5: DTA of Sewage sludge sample at 5, 10, 20°C/min

4.3 Kinetic and Thermodynamic Analysis through Model Fitting Approach:

4.3.1 Kinetic Parameters through Coats and Redfern Method:

After illustrating the pyrolysis process of sewage sludge sample, several types of kinetic models with different kinetic mechanism of pyrolysis could be further acknowledged based on TG-DTA curves. Representative mechanism functions were used to satisfy these results, as represented in Table 4.1. Appropriate model can be chosen on the basis of linear fitting of the main solid-state reaction kinetic models and the linear regression coefficient R^2 of each model. The model with the linear regression R^2 nearly equal to 0.99 could be considered as the most appropriate mechanism model. However, this is not hard and fast rule. The value of R^2 would not provide assurance that the selected reaction mechanism of pyrolysis process was best fitted or not. For this purpose, the Malek method was developed to approve the selected mechanism model[113].

Table 4.1 illustrated the kinetic parameters like activation energy, pre-exponential factor and linear regression at 5, 10 and 20°C/min. All given model provided linear regression coefficient R^2 from 0.91 to 0.99 except at 10°C/min for power law at temperature range of section I from 200 to 400°C and 5°C/min for Avrami-Erofeev equation (Nucleation and growth, N=2) at temperature range of section II at 400 to 600°C which showed poor linear regression like 0.89 and 0.85 for both models. phase interfacial reaction Shirkage geometrical Column model at 10°C/min could be considered as best fitted model based on ideal linear regression equal to 0.99 for both sections. Activation energy and pre-exponential also calculated for each reaction model at 5, 10 and 20°C/min. chemical reaction model with order two provided activation energy 25.8, 29.3 and 27.4Kj/mole for section I and 9.61, 1.31 and 1.21 kJ/mole at 5, 10, and 20°C/min. Similarly, in each model activation energy decreased at elevated temperature which means that reaction rate constant increased and speed up the reactions occurring during pyrolysis process and mass loss occur earlier.

Table 4.1: Kinetic parameters of sewage sludge sample by using different mechanism function for model fitting approach

Model Name	**Heating Rates**	**Section I(200-400°C)**			**Section II (400-600°C)**		
		Ea (kj/mole)	**R^2**	**A(min^{-1})**	**Ea (kj/mole)**	**R^2**	**A(min^{-1})**
chemical reaction (order 1) (F1)	5°C/min	25.8	0.985	47.55	9.61	0.988	44.99
	10°C/min	29.34	0.994	95.28	1.31	0.942	156.66
	20°C/min	27.4	0.979	206.96	1.21	0.982	280
Chemical Reaction (order 1.5) (F1.5)	5°C/min	0.03057	0.963	47.5	0.006024	0.997	78.333
	10°C/min	0.0357	0.967	95	1.3125	0.998	156.6
	20°C/min	0.042	0.975	206.66	3.6365	0.996	280
Parabolic law	5°C/min	48.92	0.981	52.71	10.9	0.987	44.99

(one dimensional diffusion 1D)	10°C/min	56.28	0.992	144.18	2.73	0.992	89.99
	20°C/min	54.64	0.986	259.37	3.49	0.977	159.98
Va Lensi Equation (Two dimensional diffustion, 2D)	5°C/min	52.62	0.992	55.15	16.34	0.984	78.33
	10°C/min	59.9	0.993	159.08	6.025	0.996	156.67
	20°C/min	57.6	0.985	264.53	6.52	0.995	280
Ginstling-Broushtein Equation, (Three-dimensional diffusion, 3D)	5°C/min	12.13	0.997	47.48	19.6	0.999	78.33
	10°C/min	11.75	0.995	94.99	16.73	0.999	156.66
	20°C/min	10.97	0.994	206.62	15.99	0.999	280

Avrami-Erofeev equation (Nucleation and growth, N=1.5)	5°C/min	14.09	0.976	47.45	2.24	0.915	78.33
	10°C/min	16.45	0.991	95.014	3.28	0.996	156.66
	20°C/min	15.2	0.971	206	3.25	0.997	280
Avrami-Erofeev equation (Nucleation and growth, N=2)	5°C/min	8.27	0.961	47.49	96.4	0.852	8340.5
	10°C/min	10.04	0.986	94.99	5.56	0.999	89.99
	20°C/min	15.7	0.945	206.65	1.21	0.981	280
phase interfacial reaction (Shirkage geometrical Column) (S1)	5°C/min	22.71	0.978	47.49	3.82	0.959	78.38
	10°C/min	26.33	0.991	95.06	2.1	0.992	156.66
	20°C/min	25.02	0.98	206.75	1.82	0.975	280

phase interfacial reaction (Shirkage geometrical Spherical) (S2)	5°C/min	23.72	0.981	47.51	5.61	0.977	78.38
	10°C/min	27.32	0.992	95.05	1.039	0.955	156.67
	20°C/min	25.81	0.979	206.73	0.87	0.926	280
Power law (P)	5°C/min	5.29	0.893	47.49	6.6	0.997	78.33
	10°C/min	7.13	0.965	94.99	8.65	0.999	156.67
	20°C/min	6.78	0.952	206.66	8.24	0.998	280

Pre-exponential factor increased as the heating rate increased as illustrated in Table 4.1. Pre- exponential factor at 20°C/min was 280 (min^{-1}) for almost each model in section II and was 206 (min^{-1}) for almost all models in section I. Usually A is related to the amount of times molecules will hit in the orientation necessary to cause a reaction. Calculated range of pre-exponential factor for each model was 47-206 (min^{-1}) for temperature range 200-400°C and 44-280 (min^{-1}) for temperature range 400-600°C. Zhang et al. predicted Ea and A values as 18.03KJ/mole and 1391 min-1 for the first mass loss range and 11.87 kJ/mole and 111 min-1 for the second mass loss range, respectively for sewage sludge sample obtained from municipal waste water plan[114].

Finally, it has observed in kinetic analysis that;

- Thermogravimetric based pyrolysis analysis has positive activation energy
- Pyrolysis process depends on the heating rate and temperature zones
- In every model, activation energy decreased at elevated temperature zone that means that reaction rate constant increased and speed-up the reactions occurring during pyrolysis process.
- Higher correlation coefficient suggested best suitable model for description of complex and high ash sewage sludge pyrolysis process

4.3.2 Thermodynamic Parameters through Coats and Redfern Method:

Thermodynamic parameters such as change in enthalpy (ΔH kJ/mole), change in Gibbs free energy (ΔG, kJ/mole) and change in entropy (ΔS, kJ/mole K) were calculated at 5, 10 and 20°C/min by using different type of reaction mechanism models as shown in Table 4.2. ΔH, which is a state function, reflected the absorbed or released heat at constant pressure. All models showed positive ΔH except F1.5 in section I. The positive ΔH indicated that energy from an external source is needed for the higher energy level of the reagents to their transition state. An increment in the typical concentration of solid product could be expected with an increase of endothermic reaction at the outflow of volatile gases during pyrolysis process of sewage sludge sample. A growth in the ΔH value, time for total conversion of sewage sludge pyrolysis also increased. Thus, a higher value of the change in enthalpy could alter the activity of primary reaction in pyrolysis. ΔH followed the similar pattern as activation energy increased with the increasing heating rates. ΔG revealed the total increase energy in

approach of the reagents and the formation of the activated complex. This provides a comprehensive approach to evaluate the disorder & heat flow change and its higher value represents a lower favorability of reaction [115]. Among all models, diffusion (D1, D2, D3) and phase interfacial models (S1, S2) showed higher ΔG as compared to reaction, nucleation and power law models in section I and section II. The value of ΔG decreased with the with the increase of heating rates in section II for all models which facilities the pyrolysis process of sewage sludge at higher temperatures (400 – 550 °C). The change in entropy ΔS in Table 4.2 showed negative values which confirmed the disorder of products resulted through bond dissociation was lower than initial reactants. These negative values of entropy represented that the disintegration in the activated state has a more well-organized structure than before the thermal disintegration and that the reactions in the activated state are gentler than anticipated. The ΔS from sewage sludge at various heating rates varied from - 181 J/mole to - 225 J/mole which is higher than rice straw and rice bran, - 4.13 J/mole and – 62 J/mole, respectively.

Table 4.2: Thermodynamic parameters of sewage sludge sample at 5, 10, and 20°C/min from Model Fitting Approach.

Model Name	**Heating Rate**	**Temperature Range (200-400°C)**			**Temperature Range (400-600°C)**		
		ΔH (kJ/mole)	**ΔG (kJ/mole)**	**ΔS (kJ/Kmole)**	**ΔH (kJ/mole)**	**ΔG (kJ/mole)**	**ΔS (kJ/Kmole)**
chemical reaction Order 1 (F1)	5°C/min	23.43	86.342	-0.2207	5.702	111.623	-0.2253
	10°C/min	26.97	88.235	-0.2149	-2.597	98.448	-0.2149
	20°C/min	24.8	89.679	-0.2092	-2.282	85.593	-0.2092
Chemical reaction order 1.5 (F1.5)	5°C/min	-2.333	60.575	-0.2207	-3.901	99.852	-0.2207
	10°C/min	-2.333	58.938	-0.2149	-2.595	98.452	-0.2149
	20°C/min	-2.535	62.325	-0.2092	0.1446	88.020	-0.2092
Parabolic law (one dimensional diffusion 1D)	5°C/min	46.55	109.218	-0.2198	6.99	112.913	-0.2253
	10°C/min	53.91	114.194	-0.2115	0.485	102.034	-0.2160
	20°C/min	52.06	116.337	-0.2073	-0.00188	89.828	-0.2138
Va Lensi Equation (Two dimensional diffustion, 2D)	5°C/min	50.25	122.811	-0.2546	12.432	116.186	-0.2207
	10°C/min	57.53	117.581	-0.2107	2.1169	103.162	-0.2149
	20°C/min	55.02	119.247	-0.2072	3.0281	90.903	-0.2092

Ginstling-Broushtein Equation, (Three-dimensional diffusion, 3D)	5°C/min 10°C/min 20°C/min	9.76 9.38 8.39	72.676 70.653 73.253	-0.2207 -0.2149 -0.2092	15.69 12.082 12.498	119.446 113.868 100.373	-0.2207 -0.2165 -0.2092
Avrami-Erofeev equation (Nucleation and growth, N=1.5)	5°C/min 10°C/min 20°C/min	11.72 14.08 12.62	74.637 75.352 77.491	-0.2207 -0.2149 -0.2092	-1.487 -0.6275 -0.2418	102.086 100.418 87.633	-0.2203 -0.2149 -0.2092-
Avrami-Erofeev equation (Nucleation and growth, N=2)	5°C/min 10°C/min 20°C/min	5.90 7.67 13.12	68.815 68.943 77.983	-0.2207 -0.2149 -0.2092	92.49 1.652 -2.2818	178.006 104.864 85.593	-0.1819 -0.2196 -0.2092
phase interfacial reaction (Shirkage geometrical Column) (S1)	5°C/min 10°C/min 20°C/min	20.34 23.96 22.44	83.255 85.231 87.302	-0.2207 -0.2149 -0.2092	-0.08758 -1.8075 -1.6718	103.664 99.283 86.203	-0.2207 -0.2150 -0.2092

phase interfacial reaction (Shirkage geometrical Spherical) (S2)	5°C/min	21.35	84.264	-0.2207	1.7024	105.454	-0.2207
	10°C/min	24.95	86.221	-0.2149	-2.8685	98.176	-0.2149
	20°C/min	23.23	88.092	-0.2092	-2.6218	85.253	-0.2092
Power law	5°C/min	2.92	65.853	-0.2208	2.692	106.446	-0.2207
	10°C/min	4.76	66.033	-0.2149	4.742	105.787	-0.2149
	20°C/min	4.20	69.063	-0.2092	4.7481	92.623	-0.2092

4.4 Kinetic and Thermodynamic Analysis through Model Free Approach:

4.4.1 Kinetic Parameters through Friedman, KAS, OFW and Popescu Method:

The activation energies and pre-exponential factor are kinetic parameters of sewage sludge pyrolysis, which were obtained by applying model free kinetics such as KAS, OFW, Friedman and Popescu method. In this wok, to examine connection between activation energy and conversion, model free kinetics were used. In Friedman method activation energy can be determined by using equation 3.11 which provides slopes by linear graph between 1/T and $ln\left(\frac{d\alpha}{dt}\right)$ at progressive conversion degrees depicted in figure 4.6 (a). According to KAS model according to equation 3.12, activation energy Ea can be calculated by drawing a plot of inverse of temperature and $\ln(\beta/T^2)$. Slopes obtained from Linear plot between 1/T and $\ln(\beta/T^2)$ give $-Ea/R$ at regularly growing conversion degrees. OFW method was also used to determine the activation energy by using Equation 3.10. Fig 4.6 (c) illustrates slopes through linear plot between 1/T and $\log\beta$ which give $-0.453(Ea/R)$ at progressing conversion degrees. Similarly, equation 3.13 is used to determine the activation energy from Popescu method by slope obtained through graph between $2/T_{\alpha}$-$T_{\alpha-\Delta\alpha}$ and $\ln(\beta/(T_{\alpha}-T_{\alpha-\Delta\alpha})$. Picture 4.6 (d) illustrated the linear graph at different progressive conversion degrees. Damartzis et al. predicted that conversion degrees below 2% and above 95% does not included in calculation because of short correlation values[116]. Pre-exponential factor (A) can be determined by using intercept obtained from figure 4. for all four methods. Figure 4.6 shows linear fit lines of model-free methods used and corresponding Ea and A values with R2 are reported in Table 4.3. For Popescu, an interval of $\Delta\alpha=0.005$ was used in this study. The calculated values of activation energies, and pre-exponential factor and linear regression of Friedman, KAS, OFW and Popescu methods are listed in Table 4.3. The average activation energies and pre-exponential factor determined through Friedman, KAS and OFW and Popescu methods were 128.2, 148.1, 151.6, 142.2 kJ/mol, and 1.33E+3min^{-1}, 1.98E+6$min^{-1,}$ 1.21E+6min^{-1}, 1.29E+21mn^{-1} respectively. The Values calculated from Friedman, KAS, OFW and Popescu methods were in a virtuous agreement with a standard error below 15%. This agreement authenticates the consistency of calculations and confirmed the analytical power of Friedman, KAS, OFW and Popescu methods [110].

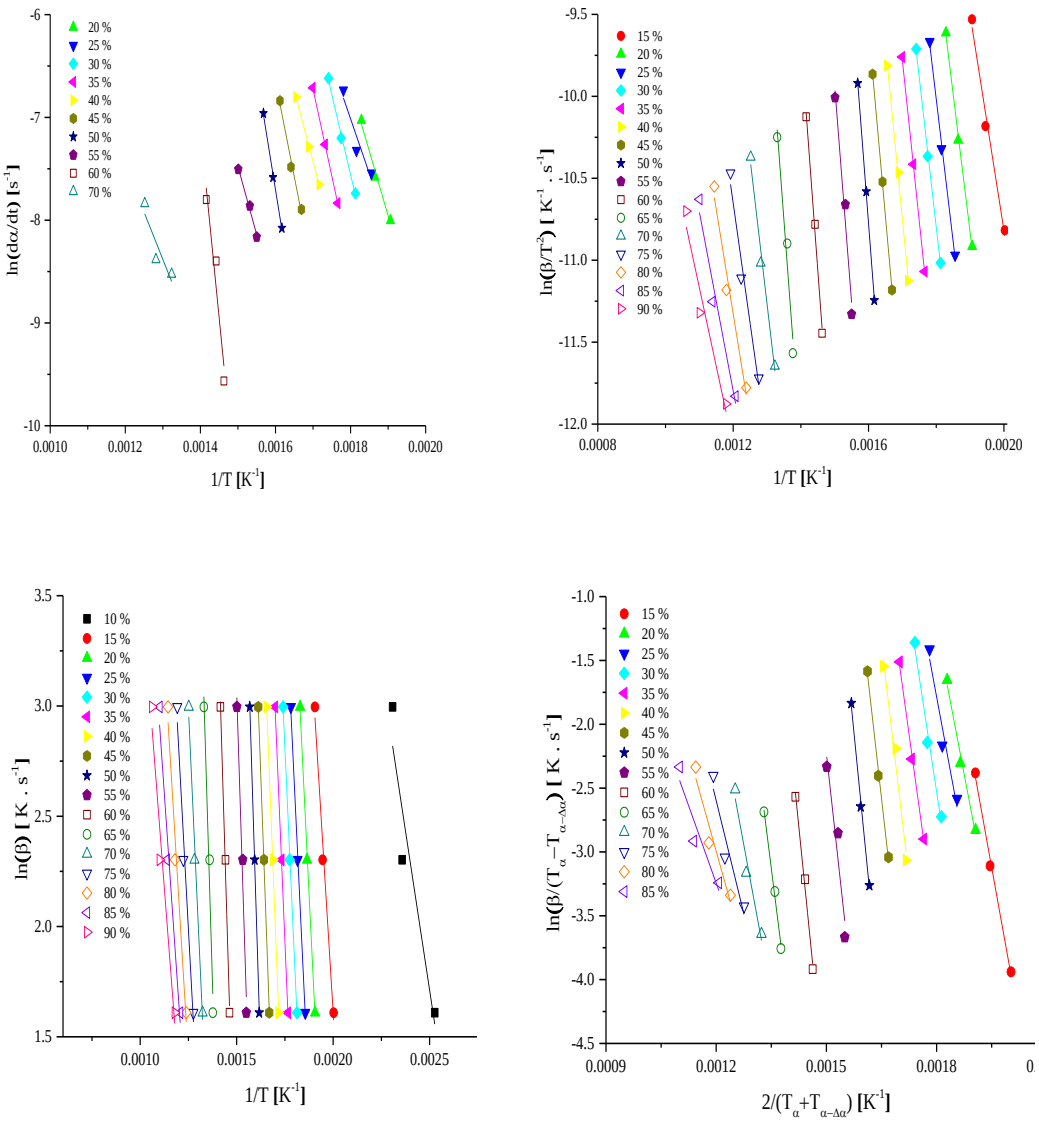

Figure 4.6: Typical linear regression lines of model free methods

Table 4.3: Kinetic Parameters Through Model Free Approach.

Conversion (α) (%)	**Friedman Method**		**OFW Method**		**KAS method**		**Popescu Method**	
	Ea (kJ/mole)-(R^2)	**A(min-1)**	**Ea (kJ/mole)-(R^2)**	**A(min-1)**	**Ea (kJ/mole)-(R^2)**	**A(min-1)**	**Ea (kJ/mole)-(R^2)**	**A(min-1)**
2.5	27.1 (0.73)	9.959E+3	54.3 (0.89)	9.632E+11	51.5 (0.86)	4.38E+08	43.6 (0.35)	1.059E+6
5.0	80.1 (0.84)	2.018E+12	84.7 (1.00)	2.375E+16	83.2 (1.00)	5.015E+4	133.5 (0.89)	3.21E+19
7.5	31.9 (0.96)	2.719E+2	62.9 (1.00)	2.313E+12	60.0 (1.00)	5.424E+4	44.1 (0.95)	7.515634
10.0	-6.9 (0.00)	3.735E+2	45.6 (0.91)	1.231E+9	41.1 (0.88)	4.955E+4	31.6 (0.69)	10.01649
12.5	10.6 (0.28)	4.553E+2	73.5 (0.94)	2.530E+11	69.3 (0.92)	1.043E+5	90.6 (0.96)	12.52161
15.0	37.7 (0.62)	5.436E+2	112.0 (0.99)	1.220E+15	109.3 (0.99)	1.973E+5	130.0 (1.00)	15.0264
17.5	92.8 (0.97)	6.344E+2	130.6 (0.99)	5.210E+16	128.6 (0.99)	2.708E+5	155.2 (1.00)	5.61E+16
20.0	104.4 (0.99)	7.245E+2	141.5 (1.00)	3.405E+5	139.9 (1.00)	3.366E+5	126.5 (0.99)	1.38E+17
22.5	103.0 (0.98)	8.145E+2	146.9 (1.00)	3.976E+6	145.4 (1.00)	3.936E+5	169.8 (1.00)	8.84E+16
25.0	88.5 (0.94)	9.04E+2	146.2 (1.00)	4.397E+5	144.6 (1.00)	4.349E+5	129.7 (0.96)	1.03E+17
27.5	138.4 (1.00)	9.943E+2	148.0 (1.00)	4.896E+5	146.4 (1.00)	4.843E+5	137.9 (0.99)	2.11E+17
30.0	129.5 (1.00)	1.084E+3	152.6 (1.00)	5.507E+5	151.1 (1.00)	5.453E+5	157.2 (0.99)	4.4E+17
32.5	127.1 (1.00)	1.174E+3	157.3 (1.00)	6.150E+5	156.0 (1.00)	6.099E+5	161.4 (1.00)	1.53E+18
35.0	140.2 (1.00)	1.264E+3	164.7 (1.00)	6.934E+5	163.6 (1.00)	6.888E+5	172.9 (1.00)	2.91E+18
37.5	131.2 (1.00)	1.354E+3	169.5 (1.00)	7.646E+5	168.6 (1.00)	7.605E+5	174.3 (0.99)	9.21E+18

40.0	114.7 (0.99)	1.444E+3	176.9 (1.00)	8.512E+5	176.2 (1.00)	8.478E+5	201.5 (0.98)	2.16E+19
42.5	136.1 (1.00)	1.534E+3	183.1 (1.00)	.361E+5	182.5 (1.00)	9.330E+5	197.3 (1.00)	8.18E+19
45.0	154.1 (0.98)	1.624E+3	191.8 (1.00)	1.038E+6	191.5 (1.00)	1.036E+6	210.9 (1.00)	1.21E+21
47.5	179.4 (1.00)	1.714E+3	207.4 (1.00)	1.185E+6	207.8 (1.00)	1.187E+6	239.5 (1.00)	1.5E+22
50.0	189.1 (1.00)	1.804E+3	222.9 (1.00)	1.340E+6	223.9 (1.00)	1.346E+6	240.3 (1.00)	2.96E+22
52.5	141.2 (0.97)	1.894E+3	230.5 (1.00)	1.455E+6	231.7 (1.00)	1.463E+6	235.0 (0.99)	1.34E+21
55.0	110.2 (1.00)	1.984E+3	219.4 (0.98)	1.451E+6	219.8 (0.98)	1.454E+6	219.0 (0.93)	1.66E+21
57.5	262.9 (0.97)	2.073E+3	226.7 (0.99)	1.567E+6	227.1 (0.99)	1.570E+6	241.0 (1.00)	1.22E+21
60.0	306.2 (0.97)	2.163E+3	231.7 (1.00)	1,672E+6	232.1 (0.99)	1.675E+6	236.2 (0.99)	1.27E+20
62.5	191.0 (1.00)	2.253E+3	225.6 (1.00)	1.696E+6	225.3 (0.99)	1.693E+6	210.3 (0.99)	9.01E+19
65.0	33.1 (0.05)	2.343E+3	230.5 (0.97)	1.802E+6	230.1 (0.97)	1.799E+6	193.8 (0.99)	6.92E+15
67.5	129.1 (0.98)	2.43E+3	179.8 (1.00)	1.459E+6	176.5 (1.00)	1.433E+6	50.7 (0.29)	3.53E+13
70.0	76.4 (0.90)	2.522E+3	151.8 (0.99)	1.278E+6	146.7 (0.99)	1.235E+6	130.1 (0.97)	2.89E+12
72.5	74.7 (0.95)	2.612E+3	139.3 (0.99)	1.214E+6	133.3 (0.99)	1.162E+6	107.4 (0.96)	3.59E+11
75.0	56.6 (0.82)	2.702E+3	128.6 (0.98)	1.160E+6	121.8 (0.98)	1.098E+6	98.5 (0.92)	3.72E+11
77.5	48.8 (0.88)	2.791E+3	121.0 (0.98)	1.128E+6	113.5 (0.98)	1.058E+6	98.0 (0.96)	8.2E+10
80.0	25.4 (0.51)	2.881E+3	114.0 (0.98)	1.097E+6	105.9 (0.98)	1.019E+6	85.9 (0.94)	2.18E+10
82.5	47.0 (0.92)	2.970E+3	106.2 (0.98)	1.053E+6	97.5 (0.97)	9.676E+5	64.5 (0.88)	5.32E+09
85.0	22.9 (0.53)	3.060E+3	100.1 (0.97)	1.023E+6	90.9 (0.97)	9.294E+5	67.5 (0.90)	1.77E+09
87.5	41.0 (0.92)	3.150E+3	94.3 (0.97)	9.925E+5	84.6 (0.96)	8.904E+5	62.9 (0.95)	6.32E+08
90.0	25.5 (0.61)	3.240E+3	90.0 (0.97)	9.743E+5	79.8 (0.95)	8.639E+5	60.9 (0.81)	2.9E+08

92.5	30.0 (0.79)	3.329E+3	85.0 (0.96)	9.458E+5	74.4 (0.95)	8.278E+5	52.6 (0.82)	81299960
95.0	14.0 (0.33)	3.419E+3	83.6 (0.96)	9.553E+5	72.6 (0.94)	8.296E+5	74.8 (0.94)	3.54E+10
97.5	92.4 (0.92)	3.509E+3	132.7 (0.99)	1.556E+6	123.6 (0.99)	1.449E+6	200.9 (1.00)	97.58724

The complete Kinetic evaluation disclosed that activation energy is vastly depended upon conversion which showed that sewage sludge pyrolysis consists of multipart process having different reactions. Figure 4.7 depicts change in activation energy with progressing conversions. For all calculated values from Friedman, KAS, OFW and Popescu model, activation energy Ea rises in the range of 2.5% to 60% conversions and decreases in the range of 60% to 95% conversion. For Friedman method activation energy abruptly raises from 27.1 to 306.2 kJ/mol. and then decreases to a value of 92.4 kJ/mol. Analogous trend has also seen in activation energy values obtained from KAS, OFW and Popescu model. Ea estimated from OFW and KAS methods agree with each other. The Ea estimated from Popescu methods contains fewer variations than those calculated from Friedman method. The Ea trends from KAS and OFW are smoother than those of other two methods. Overall, an increase in the Ea can be observed until a conversion of 60% is reached. A fall in the Ea can be seen hereafter followed by an increase after 95% of conversion. The change in activation energy with steady conversion is due to transformation in reaction mechanism. Activation energy is defined as lowest energy required to initiate a reaction, so higher activation energy values mean slower reactions.

E_a with $R^2 < 0.9$ are not included in Figure 4.7

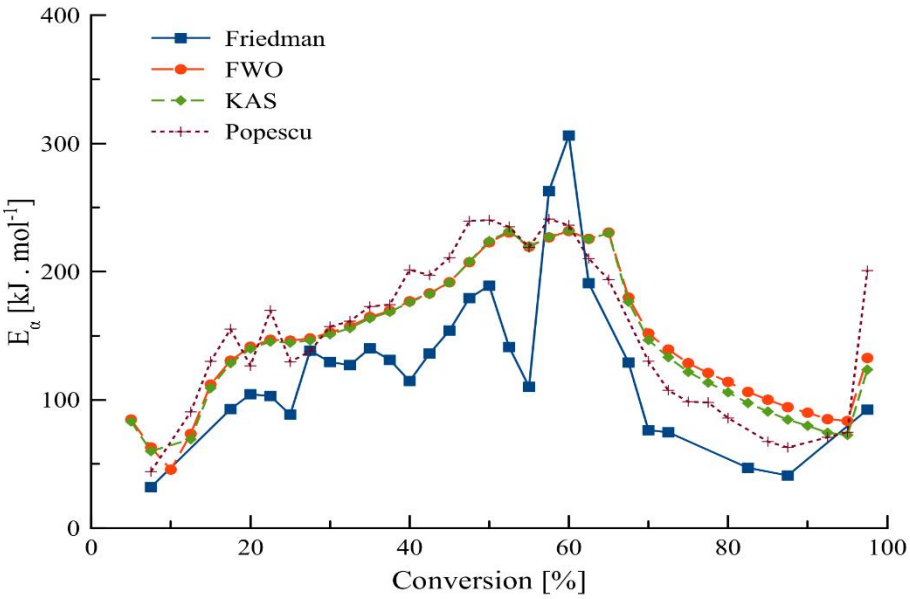

Figure 4.7: Activation energy as a function of conversion. The trends of Ea derived from different iso-conversional methods are presented in this figure.

4.4.2 Thermodynamic Parameters through Friedman, KAS, OFW and Popescu Method

Thermodynamic parameters involved Enthalpy ΔH, Gibbs free energy ΔG and entropy ΔS. These thermodynamic parameters can be calculated through maximum peak temperature Tp obtained from DTG curve of sewage sludge pyrolysis[117]. Enthalpy ΔH explain the reaction state either endothermic or exothermic with help of negative or positive sign and explain the heat exchange profile. Gibbs free energy ΔG is important thermodynamic potential and express as amount of energy required for reaction to reach the equilibrium situation. Entropy ΔS is disintegration of arranged structure of material or distortedness of material in thermodynamic system[118][119]. Entropy can be both negative or positive. All three thermodynamic parameters for Friedman, OFW, KAS and Popescu method at different conversion are given in table 4.4.

Table 4.4 illustrates that in all four methods the enthalpy is positive at each conversion which shows that at these conversions endothermic reaction occurs during pyrolysis process. The values of Gibbs free energy are also positive for all four methods. The average calculated enthalpies ΔH and Gibbs free energy for Friedman, OFW, KAS and Popescu methods are 92.32kJ/mole, 141.14kJ/mole, 137.67kJ/mole, 135.36kJ/mole and 230.18kJ/mole, 198.62kJ/mole, 208.34kJ/mole, 141.39kJ/mole. It is distinct from table that entropy is negative throughout the conversion levels. Negative entropy enlightens that the breakdown in stimulated condition has well regimented assembly than before the thermal breakdown and pyrolysis process involved disordered to well organized structure.

Table 4.4: Thermodynamic parameters of all four method with conversion.

Conversion	**Friedman Method**			**OFW method**			**KAS method**			**Popescu method**		
%	**ΔH (kJ/mole)**	**ΔG (kJ/mole)**	**ΔS (kJ/moleK)**	**ΔH (kJ/mole)**	**ΔG (kJ/mole)**	**ΔS (kJ/moleK)**	**ΔH (kJ/mole)**	**ΔG (kJ/mole)**	**ΔS (kJ/moleK)**	**ΔH (kJ/mole)**	**ΔG (kJ/mole)**	**ΔS (kJ/moleK)**
2.5	23.0348	147.2143	-0.25399	50.23512	63.88835	-0.02793	47.43512	92.37529	-0.09192	39.53512	108.9614	-0.142
5.0	76.0348	126.5093	-0.10324	80.63512	53.18071	0.056153	79.13512	160.9593	-0.16736	129.4351	72.67972	0.116083
7.5	27.8348	161.8412	-0.27409	58.83512	68.92658	-0.02064	55.93512	137.4407	-0.16671	40.03512	157.6543	-0.24057
10.0	10.9651	124.1976	-0.27645	41.53512	82.26772	-0.08331	37.03512	118.9083	-0.16746	27.53512	143.9867	-0.23818
12.5	6.53486	142.6139	-0.27833	69.43512	88.5227	-0.03904	65.23512	144.0828	-0.16127	86.53512	202.0793	-0.23633
15.0	33.6348	170.4569	-0.27985	107.9351	92.54688	0.031474	105.2351	181.4918	-0.15597	125.9351	240.7381	-0.23481
17.5	88.7348	226.1825	-0.28113	126.5351	95.88725	0.062685	124.5351	199.5048	-0.15334	151.1351	120.1856	0.063302
20.0	100.334	238.3253	-0.28224	137.4351	211.4738	-0.15143	135.8351	209.92	-0.15153	122.4351	87.81872	0.070802
22.5	98.9348	237.4041	-0.28321	142.8351	216.243	-0.15014	141.3351	214.7847	-0.15023	165.7351	132.9369	0.067083
25.0	84.4348	223.3325	-0.28409	142.1351	215.1343	-0.14931	140.5351	213.579	-0.1494	125.6351	92.23418	0.068316
27.5	134.334	273.62	-0.28488	143.9351	216.4972	-0.14841	142.3351	214.9414	-0.1485	133.8351	97.49288	0.074332
30.0	125.434	265.0737	-0.28561	148.5351	220.6192	-0.14744	147.0351	219.1594	-0.14752	153.1351	113.8189	0.080414
32.5	123.034	262.9991	-0.28627	153.2351	224.8707	-0.14652	151.9351	223.6044	-0.14659	157.3351	112.9604	0.090761
35.0	136.134	276.4003	-0.28689	160.6351	231.7826	-0.14552	159.5351	230.7099	-0.14558	168.8351	121.834	0.096133
37.5	127.134	267.6808	-0.28746	165.4351	236.1855	-0.14471	164.5351	235.3071	-0.14475	170.2351	118.5516	0.10571
40.0	110.634	251.4431	-0.288	172.8351	243.1495	-0.14382	172.1351	242.4656	-0.14385	197.4351	142.2822	0.112805

42.5	132.034	273.0896	-0.2885	179.0351	248.9631	-0.14303	178.4351	248.3764	-0.14305	193.2351	132.6739	0.123867
45.0	150.034	291.3219	-0.28898	187.7351	257.2421	-0.14216	187.4351	256.9485	-0.14218	206.8351	135.3159	0.14628
47.5	175.334	316.8417	-0.28943	203.3351	272.3045	-0.14106	203.7351	272.6967	-0.14105	235.4351	153.6871	0.167201
50.0	185.035	326.7501	-0.28985	218.8351	287.3031	-0.14004	219.8351	288.2849	-0.14	236.2351	151.7309	0.172838
52.5	137.135	279.0485	-0.29026	226.4351	294.5685	-0.13935	227.6351	295.7474	-0.13931	230.9351	159.0006	0.147129
55.0	106.135	248.2378	-0.29065	215.3351	283.4801	-0.13938	215.7351	283.8727	-0.13936	214.9351	142.1279	0.148914
57.5	258.835	401.1187	-0.29102	222.6351	290.4663	-0.13874	223.0351	290.8592	-0.13872	236.9351	165.401	0.14631
60.0	302.135	444.5918	-0.29137	227.6351	295.2047	-0.1382	228.0351	295.5977	-0.13819	232.1351	169.7714	0.127554
62.5	186.935	329.558	-0.29171	221.5351	289.0472	-0.13808	221.2351	288.7526	-0.1381	206.2351	145.2807	0.124672
65.0	29.0351	171.8175	-0.29204	226.4351	293.7005	-0.13758	226.0351	293.3075	-0.13759	189.7351	167.2968	0.045894
67.5	125.035	267.9716	-0.29235	175.7351	243.8567	-0.13933	172.4351	240.632	-0.13948	46.63512	45.65406	0.002007
70.0	72.3351	215.42	-0.29266	147.7351	216.3969	-0.14044	142.6351	211.4358	-0.14072	126.0351	135.2285	-0.0188
72.5	70.6351	213.863	-0.29295	135.2351	204.1036	-0.14086	129.2351	198.2825	-0.14122	103.3351	120.9959	-0.03612
75.0	52.5351	195.9008	-0.29323	124.5351	193.5907	-0.14124	117.7351	187.0115	-0.14169	94.43512	111.9581	-0.03584
77.5	44.7351	188.2345	-0.2935	116.9351	186.105	-0.14147	109.4351	178.865	-0.14201	93.93512	117.6005	-0.0484
80.0	21.3351	164.9639	-0.29377	109.9351	179.2181	-0.14171	101.8351	171.4177	-0.14232	81.83512	110.8952	-0.05944
82.5	42.9351	186.6893	-0.29402	102.1351	171.5811	-0.14204	93.43512	163.2285	-0.14275	60.43512	95.21928	-0.07114
85.0	18.8351	162.711	-0.29427	96.03512	165.6002	-0.14228	86.83512	156.7921	-0.14308	63.43512	102.7046	-0.08032
87.5	36.9351	180.9292	-0.29451	90.23512	159.925	-0.14254	80.53512	150.6662	-0.14344	58.83512	102.2826	-0.08886

90.0	21.4351	165.544	-0.29475	85.93512	155.7002	-0.14269	75.73512	145.9891	-0.14369	56.83512	103.4499	-0.09534
92.5	25.9351	170.1561	-0.29498	80.93512	150.8212	-0.14294	70.33512	140.7625	-0.14405	48.53512	100.3168	-0.10591
95.0	9.93511	154.2647	-0.2952	79.53512	149.3803	-0.14286	68.53512	138.9537	-0.14403	70.73512	97.81266	-0.05538
97.5	88.3351	232.7703	-0.29542	128.6351	196.4967	-0.1388	119.5351	187.6858	-0.13939	196.8351	304.0329	-0.21925

4.5 Sewage Sludge Pyrolysis in an Autoclave Reactor:

Pyrolysis yield of liquid, solid and gaseous product obtained from pyrolysis od dried sewage sludge at various temperature 350°C, 400°C and 450°C are listed in Table 4.5 The calculated values shown in the table are the mean value and the standard deviation of at least three pyrolysis runs operated at the specific temperature. It is clearly depicted in table 4.5 that as the temperature increased, the yield of liquid also increased because of primary or secondary cracking of sewage sludge components into hydrocarbons. The yield of solid char decreased at elevated temperature because solid char is converted into gaseous product at that temperature. Slow pyrolysis shifted to fast pyrolysis at elevated temperature and solid product decreased.

Table 4.5: Yield of liquid, solid and gas product obtained from sewage sludge pyrolysis at different temperature

Pyrolysis Product	**Temperature**		
	350°C	**400°C**	**450°C**
Liquid (%)	30.67	35.33	39.00
Solid (%)	58.23	55.16	51.16
Gas (%)	11.1	9.51	9.84

Gas percentage is determined by difference

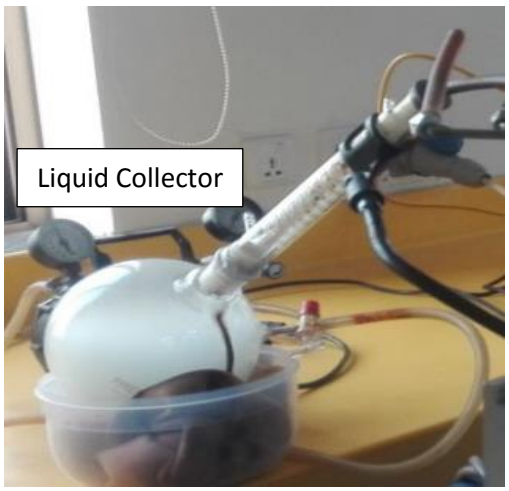

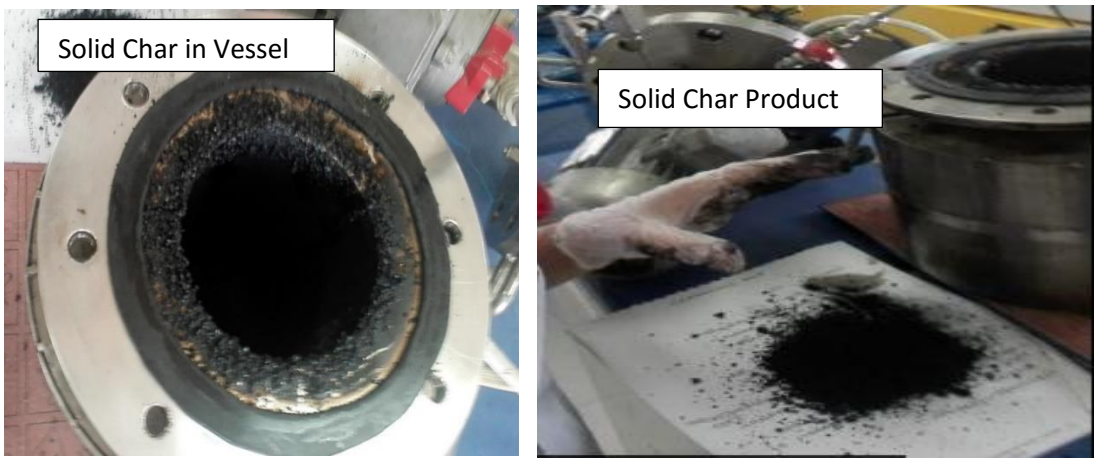

Figure 4.8: Liquid, solid and gaseous products obtained from pyrolysis of sewage sludge through autoclave pyrolyzer unit

4.6 Oil Analysis Through GC-MS:

The composition of oils obtained from pyrolysis of sewage sludge at various temperature 350°C, 400°C and 500°C was observed by GC–MS. The elements acknowledged in the fractions analyzed have been classified into six groups which were aliphatic, methyl aliphatic, aromatic and polycyclic aromatic compounds, Nitrile and amides, Alcohols and oxygen containing compounds which includes carboxylic acid, ketones and esters. Table 4.6 shows the distribution according to percentage area of various functional groups of compounds. The aliphatic compounds include alkanes, alkenes, alkynes, their derivates and compounds having carbon number from C_5 to C_{20} Like trichloro methane, pentadecane, cetane, hexadecane, Nonene and nonadecane. The aromatic and polycyclic aromatic compounds include phenol, toluene, styrene, pyrrole, benzene acetonitrile, pyridine, methylpyridine, phenols, Benzene

propanenitrile, indole and p cresol. Alcohol group contains compounds having OH group attached for example 2-Furanmethanol and 1-Dodecanol. The carboxylic acids (O=C-OH), esters (O-C=O), nitriles (C≡N) and amides (O=C-NH2) were heavy compounds linked with long aliphatic chains with carbon atoms up to 20.

Table 4.6 displays the list of Identified components and their area percentage through GC-MS of pyrolysis liquid oil obtained at 350°C, 400°C and 450°C. These components are further divided into groups based on their functional groups. Table 4.7 described that oil obtained at lower temperature contain highest percentage of aliphatic and methyl aliphatic compounds but lower percentage of aromatic, polycyclic aromatic compounds, alcoholic and heavy compounds with large molecular weight like nitrile, amides, carboxylic acid, ketones and esters. As temperature increased from 350°C to upper temperatures 400°C and 450°C the area percentage of aliphatic and methyl aliphatic compounds decreases from 90.81% and 0.62% to 85.33% and 0.55% at 400°C and 69.33% and 0.40% at 450°C. Due to temperature increase amount of aromatic, polycyclic aromatic, alcoholic compound, and heavy compounds increased.

Table 4.6: List of Identified components and their area percentage through GC-MS of pyrolysis liquid oil obtained at 350°C, 400°C and 450°C

Pyrolysis Liquid 1 at 350°C		**Pyrolysis Liquid 2 at 400°C**		**Pyrolysis Liquid 3 at 450°C**	
Name of Components	**Area %**	**Name of Components**	**Area %**	**Name of Components**	**Area %**
Methylene chloride	0.16	Trichloro methane	7.63	Silicon tetrafluoride	19.99
Ethylene chloride	30.13	Silicon tetrafluoride	22.58	Trichloro methane	43.00
Trichloro methane	57.82	Trichloro methane	51.35	Propanoic acid, 2-methyl-	1.13
Methyl Methacrylate	0.35	Propanoic acid, 2-methyl-	0.46	Pyrrole	1.89
Ethane 1,1-diethoxy-	0.40	Pyrrole	0.93	Toluene	6.62
Pyrazine	0.18	Toluene	1.00	4,4-Dimethyl-3-oxopentanenitrile	0.50
Pyrrole	0.29	Heptane, 2,4-dimethyl-	0.18	Isoamyl cyanide	1.36
Cyclotrisiloxane, hexamethyl-	0.10	Pyrazine, methyl-	0.35	2-Furanmethanol	0.30
Methyl-pyrazine	0.08	Propane, 2-bromo-2-methyl-	0.17	Ethylbenzene	1.32
Methyl-pyrazine	0.56	2,4-dimethylhept-1-ene	1.10	Styrene	0.92
4,4-Dimethyl-3-oxopentanenitrile	0.15	3-Furanmethanol	0.17	1-Nonene	0.46
Isoamyl cyanide	0.25	Styrene	0.16	Nonane	0.42
2-Furanmethanol	0.39	Pyrazine, 2,6-dimetyl-	0.17	1H-Pyrrole, 2,5-dimethyl-	0.28
Ethanone, 1-(2-furanyl)-	0.14	Phenol	0.40	Phenol	1.61
Ethane, 1,1,2,2-tetrachloro-	0.41	Cyclotetrasiloxane, octamethyl-	0.15	Cyclopropane, 1-heptyl-2-methyl-	0.40
Ethane, pentachloro-	0.17	p-Dodecyloxybenzaldehyde	0.27	Decane	0.44
Phenol	1.78	Tetra chloroethylene	0.29	1H-Pyrrole, 2-ethyl-4-methyl-	0.31
1H-Pyrazole, 4-(2-bromoethyl)-3,	0.16	Benzyl nitrile	0.20	Ethane, hexachloro-	0.42

Acetophenone	0.16	Benzene propanenitrile	0.36	p-Cresol	1.20
Ethane, hexachloro-	0.31	Indole	1.43	7-Methylthioheptanenitrile	0.34
p-Cresol	0.82	1-Dodecanol	0.21	1-Undecene	0.40
Phenol, 2-methoxy-	0.12	Tridecane	0.18	Tridecane	0.28
Phenol, 4-ethyl-	0.15	Indole, 3-methyl-	0.27	Benzyl nitrile	0.47
Benzene propane nitrile	0.20	Pentadecane	0.27	Tridecane	0.33
Indole	0.66	Cetane	0.14	Benzene propanenitrile	0.71
Tridecane	0.17	Pentadecane	0.34	Indole	2.33
Pentadecane	0.29	Hexadecane	0.29	1-Dodecanol	0.54
Hexadecane	0.26	Hexadecane	0.32	Tridecane	0.47
Nonadecane	0.28	Pentadecane, 2,6,10,14-tetramethyl	0.17	Indole, 3-methyl-	0.60
Hexadecane	0.20	Nonadecane	0.22	1-Tridecene	0.29
Pyrrolo[1,2-a] pyrazine-1,4-dione	0.21	Hexadecanenitrile	0.21	Pentadecane	0.42
Nonadecane	0.26	Nonadecane	0.34	Cetane	0.38
5,10-Diethoxy-2,3,7,8-tetrahydro-	1.24	5,10-Diethoxy-2,3,7,8-tetrahydro-	1.19	Pentadecane	0.61
Pyrrolo[1,2-a]pyrazine-1,4-dione,	0.20	Heneicosane	0.36	1-Pentadecene	0.37
Heptadecane, 2,6,10,15-tetramethyl	0.17	Heneicosane	0.39	Hexadecane	0.41
Penta decane nitrile	0.35	Hexadecanenitrile	0.41	Nonadecane	0.28
Di-n-octyl phthalate	0.51	Heneicosane	0.27	Hexadecanenitrile	0.33
		Heneicosane	0.22	1-Heptadecene	0.34

		Heneicosane	0.14	Pentadecanenitrile	1.44
		Triphenylphosphine oxide	1.98	5,10-Diethoxy-2,3,7,8-tetrahydro-	0.49
		1-Hexanol, 2-ethyl-	0.29	Oleanitrile	0.31
		5.beta.-Cholestan-3.alpha.-ol, trifluoroacetate	0.44	Heptadecanenitrile	0.65
		5.beta.-Cholestan-3.alpha.-ol, trifluoroacetate	0.27	Pentadecanenitrile	0.50
		5.beta.-Cholestan-3.alpha.-ol, trifluoroacetate	0.52	5.beta.-Cholestan-3.alpha.-ol, trifluoroacetate	1.18
		Cholestane	0.19	5.beta.-Cholestan-3.alpha.-ol, trifluoroacetate	0.78
		Cholest-4-ene	0.15	Cholest-4-ene	0.48
		Cholesta-3,5-diene	0.17	5.beta.-Cholestan-3.alpha.-ol, trifluoroacetate	0.63
		Cholestan-3-ol, (3.alpha.,5.beta.)-	0.20	Cholesta-3,5-diene	0.32
		5-.alpha.-Androst-2-en-17-.beta.-ol	0.23	5.beta.-Cholestan-3.alpha.-ol, trifluoroacetate	0.41
		Stigmastane, 23,24-epoxy-, (5.alp	0.27	5-.alpha.-Androst-2-en-17-.beta.-ol, 17-methyl-	0.32

Table 4.7: Classification according to area percentage of the different functional group of compounds in the chromatographed elements of the pyrolysis oils at different temperature

Functional group	**Pyrolysis Liquid 1 at 350°C**	**Pyrolysis Liquid 2 at 400°C**	**Pyrolysis Liquid 3 at 450°C**
Aliphatic	90.81%	85.33%	69.33%
Methyl Aliphatic	0.62%	0.55%	0.40%
Aromatic and polycyclic aromatic	7.23%	10.11%	17.77%
Nitrile and amides	0.65%	1.18%	5.43%
Alcohol	0.39%	2.37%	5.45%
Ketone, Ester and acids	0.30%	0.46%	1.62%

4.7 Gas Analysis Through GC-TCD:

Table 4.8 illustrated the area percentage of non-condensable gases (hydrogen H_2, methane CH_4, carbon monoxide CO and carbon dioxide CO_2) obtained from GC-TCD analysis of gaseous product from the sewage sludge pyrolysis trough autoclave pyrolyzer unit with char and liquid oil product at different temperatures at 350°C, 400°C and 450°C. Carbon monoxide CO and hydrogen H_2 has highest percentage area among all other gases at all temperature. According to these results, the combined percentage of H_2+CO (synthetic gas) is much higher from methane CH_4 and carbon dioxide CO_2 obtained from pyrolysis of dried sewage sludge by using autoclave pyrolyzer unit at 350°C, 400°C and 450°C temperatures.

Figure 4.9 depicted the relationship of temperature and area percentage of gaseous product through GC-TCD analysis. This graph represented that as the temperature increased from 350°C to 400°C and 450°C the area percentage of carbon monoxide CO increased from 20.93% to 26.44% and 28.94%. Area percentage of methane and carbon dioxide also increased as the temperature increased and area percentage of

hydrogen decreased. Remaining percentage is indication of presence of N_2, O_2, C_2H_4, C_2H_6 and ΣC_xH_y which is not identified due to low residence time limits of detector used.

Table 4.8: Classification according to area percentage of the different gases present in pyrolysis gas obtained at different temperature.

Name of Gas	Gas at 350°C	Gas at 400°C	Gas at 450°C
Hydrogen H_2	7.68%	3.68%	0.074%
Methane CH_4	0.98%	2.20%	3.14%
Carbon monoxide CO	20.93%	26.44%	28.94%
Carbon dioxide CO_2	0.26%	1.02%	2.02%

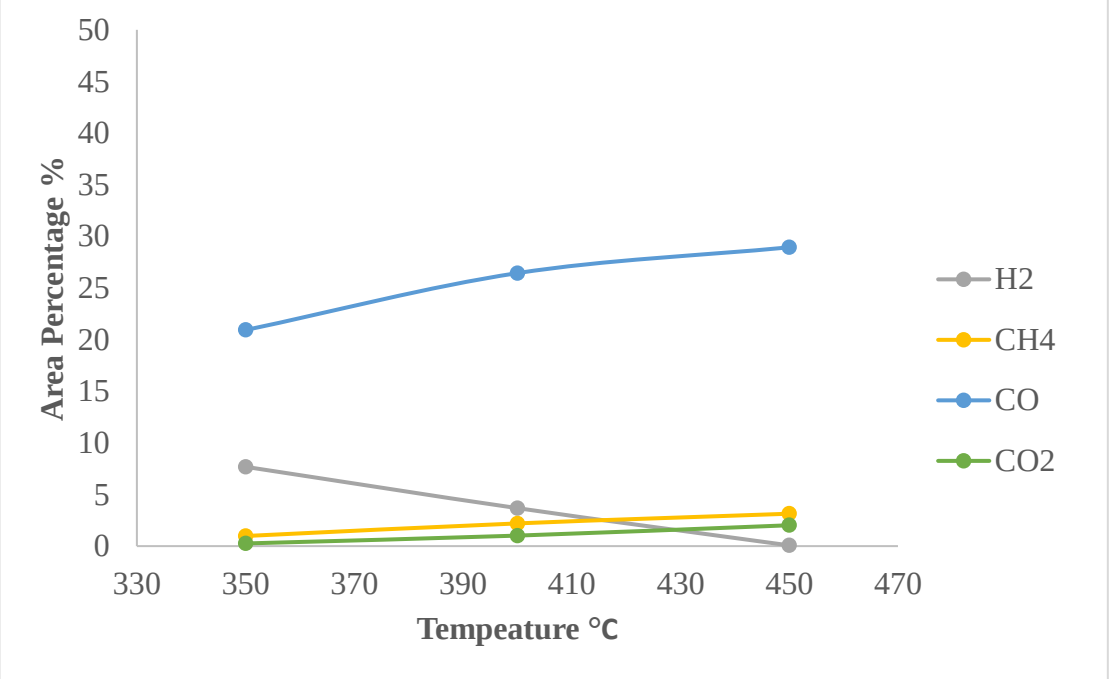

Figure 4.9: Effect of temperature on area percentage % of different gases analyzed by GC-TCD

4.8 Thermogravimetric Analysis of Char:

4.8.1 TGA of Char:

Figure 4.10 depicted the TGA curve of pure sewage sludge, char 1, char 2 and char 3 obtained from pyrolysis process of dried sewage sludge through autoclave pyrolyzer unit at temperature at 350°C, 400°C and 450°C respectively at 10°C/min.

It is clearly shown that thermal decomposition profile of these materials is divided into three steps, one is dehydration, other is devolatilization and combustion phase and last one is burnout phase. For sewage sludge, char 1 obtained at 350°C, Char 2 obtained at 400°C and char 3 at 450°C, all has dehydration phase from room temperature up to 150°C. For sewage sludge devolatilization phase is from 200°C to 400°C and combustion phase is from 400 to 600°C. The range above 600°C is burnout phase.

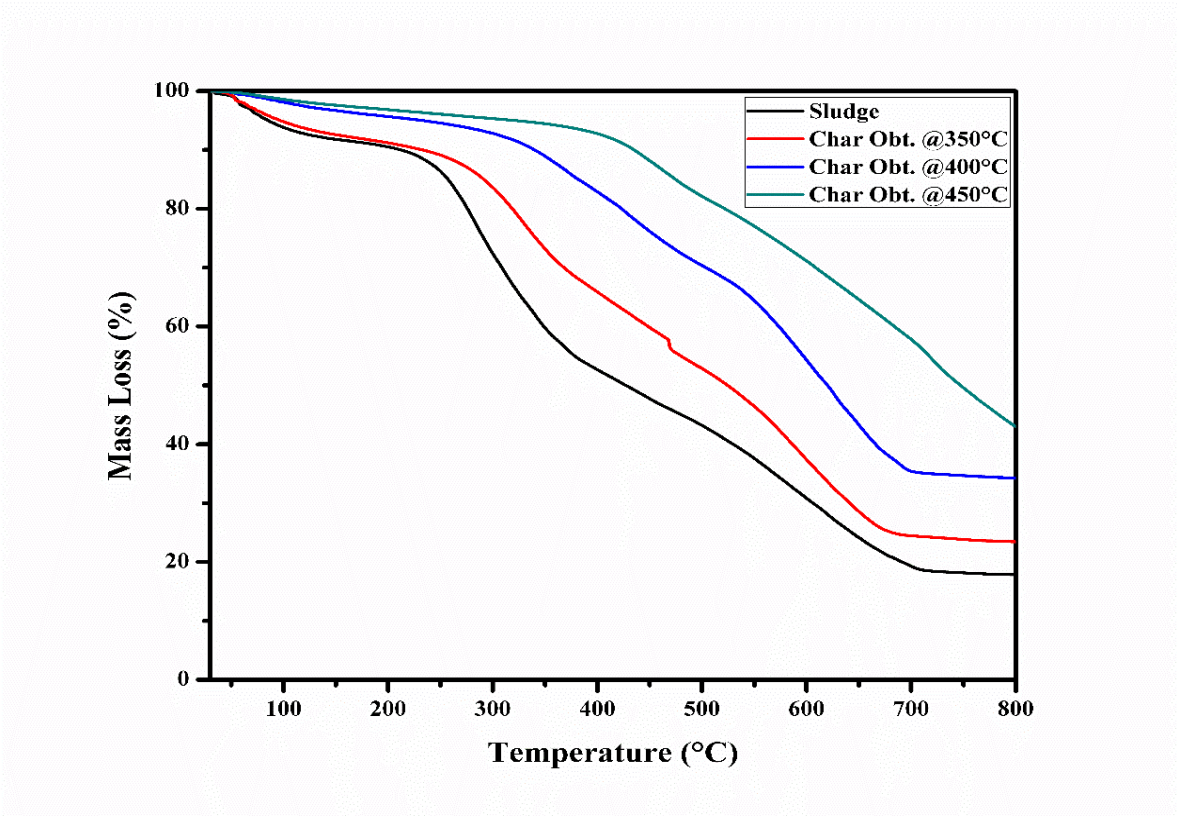

Figure 4.10: TGA curves of pure sewage sludge, char 1 obtained at 350^{o}C, Char 2 obtained at 400^{o}C, and char 3 obtained at 450^{o}C

For char 1 at 350°C devolatilization phase from 300°C TO 450°C and combustion phase is from 450°C to 650°C and above 650°C is burnout phase. For char 2 obtained at 400°C, devolatilization phase is from 350°C to 500°C and combustion phase is from

500°C to 700°C and above 700°C is burn out phase for this. Char 3 obtained at 400°C has very negligible volatilization phase and combustion phase to 700°C.

It is evidently shown from TGA curves that 100% sewage sludge started disintegrates first and then char 1, char 2 and char 3 respectively in main devolatilization and combustion zone because char obtained from sewage sludge contain elements which is organized in macro-molecular structure. These components are associated together with comparatively strong bonds than that of bonds in sewage sludge components that break at elevated temperature[120].

4.8.2 DTA of Char:

Figure 4.11 depicted the Differential thermogravimetric analysis DTA of pure sewage sludge, char 1, char 2 and char 3 obtained from pyrolysis process of dried sewage sludge through autoclave pyrolyzer unit at temperature at 350°C, 400°C and 450°C respectively at 10°C/min.

It provides information about the heat loss or gain during disintegration process and indicated about reaction either endothermic or exothermic. It also predicts the temperature at which the maximum mass loss occurs. It also gives information about percentage mass loss as each stage[111][112].

Initially pure sewage sludge decomposes through endothermic reactions gives maximum conversion at 97°C with 6% mass loss respectively. Char 1 at 350°C, Char at 400°C and char at 450°C give endothermic reaction at maximum conversion temperature at 80°C, 85°C and 90°C with 6%, 5.5% and 5% mass loss due to removal of moisture content and lighter components.

As temperature rises from 200°C the decomposition reactions converted from endothermic reactions to exothermic reaction. In main devolatilization and combustion phase, Pure sewage sludge give maximum conversion at temperature 470°C with 55% mass loss. Char 1, char 2 and char 3 contain maximum conversion at 480°C, 510°C and 530°C with 35%, 40% and 50% mass loss.

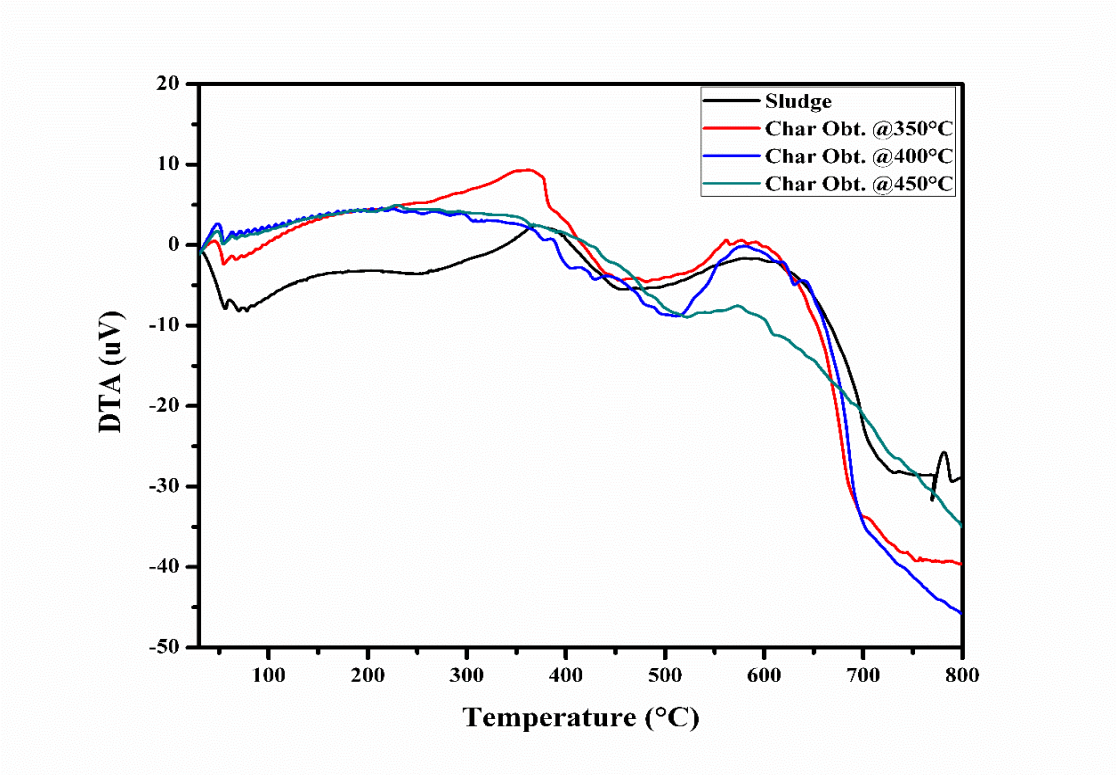

Figure 4.11: DTA curves of pure sewage sludge, char 1 obtained at 350^{o}C, char 2 obtained at 400^{o}C, char 3 obtained at 450^{o}C

4.9 FTIR Analysis of Char:

The spectra of FTIR analysis reveals discernable deviations during pyrolysis that are related to the temperature change. Figure 4.12 displays detailed spectral progression with pyrolysis for selected wavenumber ranges. Generally, the organic functional groups found in sewage sludge lean towards to decrease or even disappear as pyrolysis temperature increases. Upon nearer inspection, some structural fluctuations in the solid product can be distinguished.

For instance, pyrolytic breakdown of O-H or N-H group in the range of 3600-3200cm^{-1} takes a noticeable consequence as the temperature increased from 350°C to 450°C. This Structure of spectra is clearly visible for sewage sludge and Char 1 at 350°C but the spectral peak at this range is not present for char 3 at higher temperature 450°C, thus confirming that the disintegration of the hydrogen based fraction is complete at 350°C.

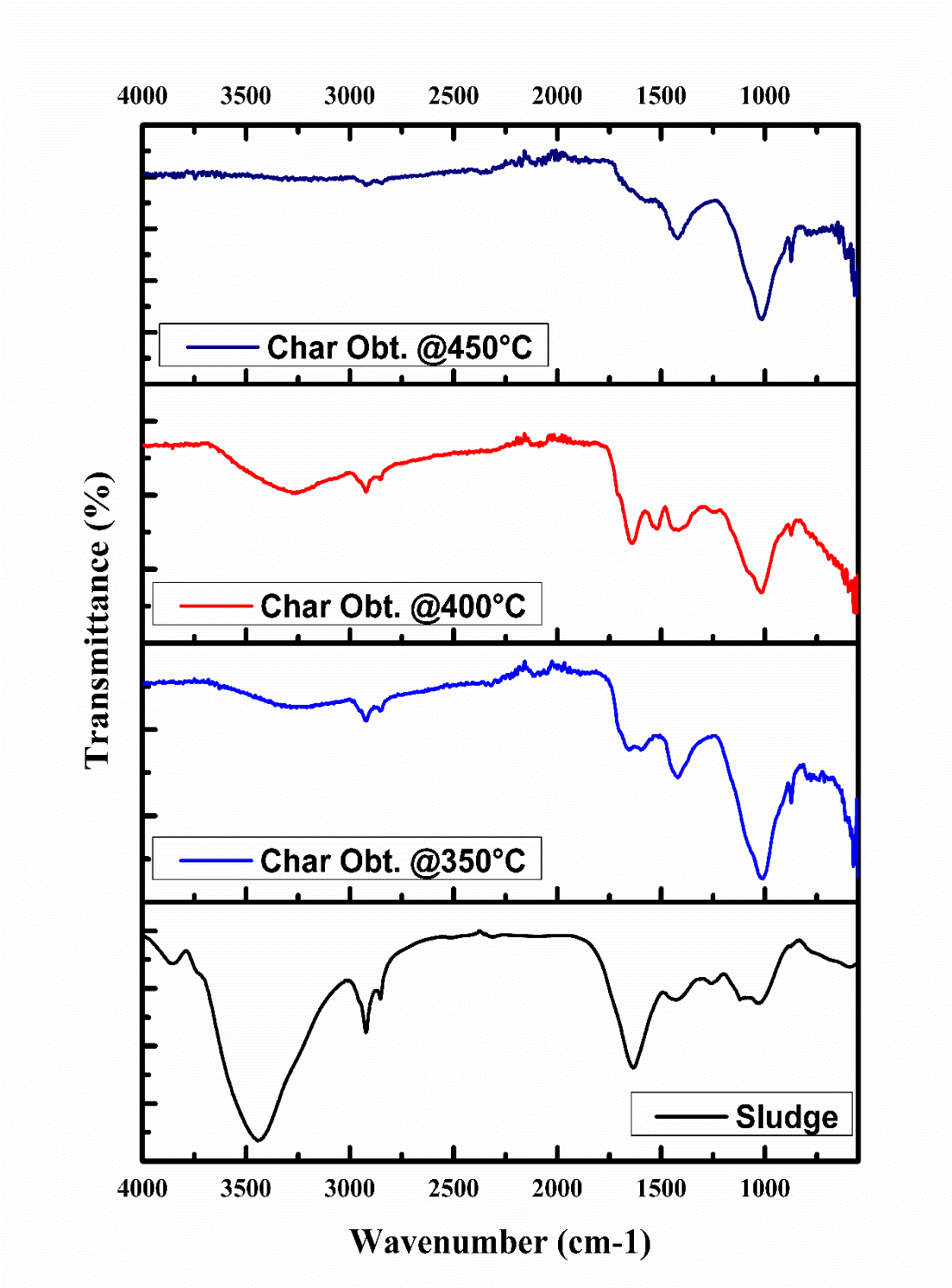

Figure 4.12: FTIR curves of pure sewage sludge, char 1 obtained at 350°C, char 2 obtained at 400°C, char 3 obtained at 450°C

Chapter 5

Conclusion and Future Recommendation

5.1 Conclusion:

Thermal degradation behavior in pyrolysis process of sewage sludge was carried out by using a lab scale autoclave pyrolyzer unit and thermogravimetric analysis. Sewage sludge sample in dried and powdered form was used for all treatments. Thermodynamic and kinetic parameters through model free and model fitting kinetics were also analyzed in this research. Pyrolysis products (bio-oil, char and gaseous products) were investigated as well to compare the quality.

The sewage sludge sample contained higher percentage of volatile matters 44.6%, ash 44.6%, carbon 40.4% and oxygen 45.7% on dry basis. These proportions of volatiles in sample favors for thermal degradation processes because desirable products could be obtained by utilizing such material. FTIR analysis of sewage sludge exposed identification of amides, aldehydes, Nitriles, aromatic derivatives and carboxylic groups.

Different model free and model fitting kinetic methods for kinetic and thermodynamic parameters calculation were investigated in this study by using thermogravimetric data to analyze the nature of reaction characteristics of sewage sludge pyrolysis. TGA and DTA curves of sewage sludge pyrolysis were analyzed and two phases were identified: phase 1 from 200 to 400 °C and phase 2 from 400 – 600°C. In model fitting approach, Shirkage geometrical Column model at 10°C/min could be considered as best fitted model based on ideal linear regression equal to 0.99 for both sections. In model free kinetics, for all calculated values from Friedman, KAS, OFW and Popescu model, activation energy Ea rises in the range of 2.5% to 60% conversions and decreases in the range of 60% to 95% conversion. For Friedman method activation energy abruptly raises from 27.1 to 306.2 kJ/mol. and then decreases to a value of 92.4 kJ/mol and in all four methods the enthalpy is positive at each conversion which shows that at these conversions endothermic reaction occurs during pyrolysis process. The values of

Gibbs free energy and entropy are positive and negative respectively for all four methods.

The influence of the reaction temperature (350 –450°C) on products yield and characteristics in lab scale pyrolysis process was considered. The highest bio-oil yield of 39 weight % was attained at the pyrolysis temperature of 450°C. Biochar and gaseous product yield showed declining profile with increment of pyrolysis temperature.

5.2 Future Recommendations:

Based on the above results, for more exploring in pyrolysis process, the following future work is recommended:

- The design amendment in pyrolyzer unit in terms of high production liquid fuel could be prolonged by providing new techniques and optimum process condition such as temperature, nature of feedstock and residence time.

- A computational model should be established to enhance the physical, chemical and reaction parameters which will help to design the process.

- Different kinetic model should be established to investigate the best functioning condition to design the pyrolysis process to obtain the maximum yield with lower investment.

- It should be developed on commercial scale because Sewage sludge can be better alternative for fossil fuels, thermal degradation can reduce environmental hazards, usage of catalyst and reagent can be reduced, bio fuel quality can be upgraded

References:

[1] "World Energy Outlook 1998."

[2] "Sewage sludge production and disposal - Eurostat." [Online]. Available: http://ec.europa.eu/eurostat/web/products-datasets/product?code=env_ww_spd. [Accessed: 12-Dec-2017].

[3] M. Atienza-Martínez, J. F. Mastral, J. Ábrego, J. Ceamanos, and G. Gea, "Sewage Sludge Torrefaction in an Auger Reactor," *Energy & Fuels*, vol. 29, no. 1, pp. 160–170, Jan. 2015.

[4] C. He, K. Wang, Y. Yang, and J.-Y. Wang, "Utilization of Sewage-Sludge-Derived Hydrochars toward Efficient Cocombustion with Different-Rank Coals: Effects of Subcritical Water Conversion and Blending Scenarios," *Energy & Fuels*, vol. 28, no. 9, pp. 6140–6150, Sep. 2014.

[5] A. Christodoulou and K. Stamatelatou, "Overview of legislation on sewage sludge management in developed countries worldwide," *Water Sci. Technol.*, vol. 73, no. 3, pp. 453–462, Feb. 2016.

[6] P. Manara and A. Zabaniotou, "Towards sewage sludge based biofuels via thermochemical conversion – A review," *Renew. Sustain. Energy Rev.*, vol. 16, no. 5, pp. 2566–2582, Jun. 2012.

[7] D. Fytili and A. Zabaniotou, "Utilization of sewage sludge in EU application of old and new methods—A review," *Renew. Sustain. Energy Rev.*, vol. 12, no. 1, pp. 116–140, Jan. 2008.

[8] A. Raheem, M. Y. Hassan, and R. Shakoor, "Bioenergy from anaerobic digestion in Pakistan: Potential, development and prospects," *Renew. Sustain. Energy Rev.*, vol. 59, pp. 264–275,

Jun. 2016.

[9] B. Khiari, F. Marias, F. Zagrouba, and J. Vaxelaire, “Analytical study of the pyrolysis process in a wastewater treatment pilot station,” *Desalination*, vol. 167, pp. 39–47, Aug. 2004.

[10] M. Inguanzo, A. Domínguez, J. . Menéndez, C. . Blanco, and J. . Pis, “On the pyrolysis of sewage sludge: the influence of pyrolysis conditions on solid, liquid and gas fractions,” *J. Anal. Appl. Pyrolysis*, vol. 63, no. 1, pp. 209–222, Mar. 2002.

[11] B. Zhang, S. Xiong, B. Xiao, D. Yu, and X. Jia, “Mechanism of wet sewage sludge pyrolysis in a tubular furnace,” *Int. J. Hydrogen Energy*, vol. 36, no. 1, pp. 355–363, Jan. 2011.

[12] J. . Menéndez, M. Inguanzo, and J. . Pis, “Microwave-induced pyrolysis of sewage sludge,” *Water Res.*, vol. 36, no. 13, pp. 3261–3264, Jul. 2002.

[13] P. Morf, P. Hasler, and T. Nussbaumer, “Mechanisms and kinetics of homogeneous secondary reactions of tar from continuous pyrolysis of wood chips,” *Fuel*, vol. 81, no. 7, pp. 843–853, May 2002.

[14] J. Shao, R. Yan, H. Chen, B. Wang, D. H. Lee, and D. T. Liang, “Pyrolysis Characteristics and Kinetics of Sewage Sludge by Thermogravimetry Fourier Transform Infrared Analysis †,” *Energy & Fuels*, vol. 22, no. 1, pp. 38–45, Jan. 2008.

[15] W.-T. Tsai, M.-K. Lee, J.-H. Chang, T.-Y. Su, and Y.-M. Chang, “Characterization of bio-oil from induction-heating pyrolysis of food-processing sewage sludges using chromatographic analysis,”

Bioresour. Technol., vol. 100, no. 9, pp. 2650–2654, May 2009.

[16] S. Xiong, B. Zhang, X. Jia, B. Xiao, and M. He, "Feasibility Study on the Pyrolysis Production for Hydrogen-Riched Fuel Gas from the Wet Sewage Sludge," in *2009 3rd International Conference on Bioinformatics and Biomedical Engineering*, 2009, pp. 1–4.

[17] M. E. Sánchez *et al.*, "Effect of pyrolysis temperature on the composition of the oils obtained from sewage sludge," *Biomass and Bioenergy*, vol. 33, no. 6–7, pp. 933–940, Jun. 2009.

[18] J. . Conesa, A. Marcilla, R. Moral, J. Moreno-Caselles, and A. Perez-Espinosa, "Evolution of gases in the primary pyrolysis of different sewage sludges," *Thermochim. Acta*, vol. 313, no. 1, pp. 63–73, Mar. 1998.

[19] M. Yahiaoui, H. Hadoun, I. Toumert, and A. Hassani, "Determination of kinetic parameters of Phlomis bovei de Noé using thermogravimetric analysis," *Bioresour. Technol.*, vol. 196, pp. 441–447, Nov. 2015.

[20] J. F. Saldarriaga, R. Aguado, A. Pablos, M. Amutio, M. Olazar, and J. Bilbao, "Fast characterization of biomass fuels by thermogravimetric analysis (TGA)," *Fuel*, vol. 140, pp. 744–751, Jan. 2015.

[21] L. Sanchez-Silva, D. López-González, A. M. Garcia-Minguillan, and J. L. Valverde, "Pyrolysis, combustion and gasification characteristics of Nannochloropsis gaditana microalgae," *Bioresour. Technol.*, vol. 130, pp. 321–331, Feb. 2013.

[22] M. A. Islam, M. Auta, G. Kabir, and B. H. Hameed, "A

thermogravimetric analysis of the combustion kinetics of karanja (Pongamia pinnata) fruit hulls char," *Bioresour. Technol.*, vol. 200, pp. 335–341, Jan. 2016.

[23] Q.-V. Bach, K.-Q. Tran, and Ø. Skreiberg, "Comparative study on the thermal degradation of dry- and wet-torrefied woods," *Appl. Energy*, vol. 185, pp. 1051–1058, Jan. 2017.

[24] Q.-V. Bach and W.-H. Chen, "A comprehensive study on pyrolysis kinetics of microalgal biomass," *Energy Convers. Manag.*, vol. 131, pp. 109–116, Jan. 2017.

[25] "Review of fast pyrolysis of biomass and product upgrading," *Biomass and Bioenergy*, vol. 38, pp. 68–94, Mar. 2012.

[26] S. Rapagnà, N. Jand, and P. U. Foscolo, "Catalytic gasification of biomass to produce hydrogen rich gas," *Int. J. Hydrogen Energy*, vol. 23, no. 7, pp. 551–557, Jul. 1998.

[27] D. Mohan, A. Charles U. Pittman, Jr., and P. H. Steele, "Pyrolysis of Wood/Biomass for Bio-oil: A Critical Review," 2006.

[28] I. Fonts, G. Gea, M. Azuara, J. Ábrego, and J. Arauzo, "Sewage sludge pyrolysis for liquid production: A review," *Renew. Sustain. Energy Rev.*, vol. 16, no. 5, pp. 2781–2805, 2012.

[29] M. C. Samolada and A. A. Zabaniotou, "Comparative assessment of municipal sewage sludge incineration, gasification and pyrolysis for a sustainable sludge-to-energy management in Greece," *Waste Manag.*, vol. 34, no. 2, pp. 411–420, 2014.

[30] X. Rongzhen, "Study on Resource Reuse of Municipal Sewage Sludge," *]. Environ. Sci. Manag.*, vol. 35(2), pp. 82–84, 2008.

[31] S. Inoue, S. Sawayama, T. Ogi, and S. Yokoyama, “Organic composition of liquidized sewage sludge,” *Biomass and Bioenergy*, vol. 10, no. 1, pp. 37–40, 1996.

[32] Y. D. He *et al.*, “The fate of Cu, Zn, Pb and Cd during the pyrolysis of sewage sludge at different temperatures,” *Environ. Technol.*, vol. 31, no. 5, pp. 567–574, 2010.

[33] E. Agrafioti, G. Bouras, D. Kalderis, and E. Diamadopoulos, “Biochar production by sewage sludge pyrolysis,” *J. Anal. Appl. Pyrolysis*, vol. 101, pp. 72–78, 2013.

[34] C. Briens, J. Piskorz, and F. Berruti, “Biomass Valorization for Fuel and Chemicals Production -- A Review,” *Int. J. Chem. React. Eng.*, vol. 6, no. May 2008, pp. 1–49, 2008.

[35] I. Fonts, M. Azuara, G. Gea, and M. B. Murillo, “Study of the pyrolysis liquids obtained from different sewage sludge,” *J. Anal. Appl. Pyrolysis*, vol. 85, no. 1–2, pp. 184–191, 2009.

[36] D. J. Bushnell, C. Haluzok, and A. Dadkhah-Nikoo, “Biomass Fuel Characterization : Testing and Evaluating the Combustion Characteristics of Selected Biomass Fuels : Final Report May 1, 1988-July, 1989.,” Portland, OR, Apr. 1990.

[37] A. Demirbas, “Calculation of higher heating values of fatty acids,” *Energy Sources, Part A Recover. Util. Environ. Eff.*, vol. 38, no. 18, pp. 2693–2697, 2016.

[38] X. Xu *et al.*, “Co-pyrolysis characteristics of municipal sewage sludge and hazelnut shell by TG-DTG-MS and residue analysis,” *Waste Manag.*, vol. 62, pp. 91–100, 2017.

[39] N. Ruiz-Gómez, V. Quispe, J. Ábrego, M. Atienza-Martínez, M. B. Murillo, and G. Gea, “Co-pyrolysis of sewage sludge and manure,” *Waste Manag.*, vol. 59, pp. 211–221, 2017.

[40] K. Wang, Y. Zheng, X. Zhu, C. E. Brewer, and R. C. Brown, “Ex-situ catalytic pyrolysis of wastewater sewage sludge – A micro-pyrolysis study,” *Bioresour. Technol.*, vol. 232, pp. 229–234, 2017.

[41] J. Alvarez *et al.*, “Characterization of the bio-oil obtained by fast pyrolysis of sewage sludge in a conical spouted bed reactor,” *Fuel Process. Technol.*, vol. 149, pp. 169–175, 2016.

[42] H. Fan and K. He, “Fast Pyrolysis of Sewage Sludge in a Curie-Point Pyrolyzer : The Case of Sludge in the City of Shanghai , China,” 2016.

[43] Y. Huang, C. Shih, P. Chiueh, and S. Lo, “Microwave co-pyrolysis of sewage sludge and rice straw,” *Energy*, vol. 87, pp. 638–644, 2015.

[44] J. Alvarez, M. Amutio, G. Lopez, I. Barbarias, J. Bilbao, and M. Olazar, “Sewage sludge valorization by flash pyrolysis in a conical spouted bed reactor,” *Chem. Eng. J.*, vol. 273, pp. 173–183, 2015.

[45] P. Taylor, “pt us,” no. August, pp. 37–41, 2014.

[46] Q. Xie *et al.*, “Bioresource Technology Fast microwave-assisted catalytic pyrolysis of sewage sludge for bio-oil production,” *Bioresour. Technol.*, vol. 172, pp. 162–168, 2014.

[47] N. Gao, J. Li, B. Qi, A. Li, Y. Duan, and Z. Wang, “Journal of Analytical and Applied Pyrolysis Thermal analysis and products distribution of dried sewage sludge pyrolysis,” *J. Anal. Appl.*

Pyrolysis, vol. 105, pp. 43–48, 2014.

[48] W. Zuo, B. Jin, Y. Huang, and Y. Sun, “Characterization of top phase oil obtained from co-pyrolysis of sewage sludge and poplar sawdust,” 2014.

[49] J. Cao, L. Li, K. Morishita, X. Xiao, X. Zhao, and X. Wei, “Nitrogen transformations during fast pyrolysis of sewage sludge,” *Fuel*, vol. 104, pp. 1–6, 2013.

[50] S. Xiong, J. Zhuo, B. Zhang, and Q. Yao, “Journal of Analytical and Applied Pyrolysis Effect of moisture content on the characterization of products from the pyrolysis of sewage sludge,” *J. Anal. Appl. Pyrolysis*, vol. 104, pp. 632–639, 2013.

[51] S. Hu *et al.*, “Characterization of char from rapid pyrolysis of rice husk,” *Fuel Process. Technol.*, vol. 89, no. 11, pp. 1096–1105, 2008.

[52] T. Karayildirim, J. Yanik, M. Yuksel, and H. Bockhorn, “Characterisation of products from pyrolysis of waste sludges,” vol. 85, pp. 1498–1508, 2006.

[53] G. Mishra, J. Kumar, and T. Bhaskar, “Bioresource Technology Kinetic studies on the pyrolysis of pinewood,” *Bioresour. Technol.*, vol. 182, pp. 282–288, 2015.

[54] A. Olajire, C. Zhi, S. Hanson, and C. Wai, “Thermogravimetric analysis of the pyrolysis characteristics and kinetics of plastics and biomass blends,” *Fuel Process. Technol.*, vol. 128, pp. 471–481, 2014.

[55] N. Scotia, “Determination of Reaction Kinetics of Wheat Straw

Using Thermogravimetric Analysis," vol. 34, no. 1, 1992.

[56] W. Rulkens, "Sewage Sludge as a Biomass Resource for the Production of Energy : Overview and Assessment of the Various Options †," vol. 44, no. 1, pp. 9–15, 2008.

[57] R. Font, A. Fullana, and J. Conesa, "Kinetic models for the pyrolysis and combustion of two types of sewage sludge," vol. 74, pp. 429–438, 2005.

[58] S. A. Scott, J. S. Dennis, J. F. Davidson, and A. N. Hayhurst, "Thermogravimetric measurements of the kinetics of pyrolysis of dried sewage sludge," vol. 85, pp. 1248–1253, 2006.

[59] H. Im and C. Gyu, "Characterization of dried sewage sludge for co-firing in coal power plant by using thermal gravimetric analysis," *J. Mater. Cycles Waste Manag.*, vol. 0, no. 0, p. 0, 2017.

[60] F. Okonta, N. Freeman, and A. Bel, "Thermal decomposition of sewage sludge under N 2 , CO 2 and air : Gas characterization and kinetic analysis n Hern a," vol. 196, pp. 560–568, 2017.

[61] T. Kan, V. Strezov, and T. Evans, "E ff ect of the Heating Rate on the Thermochemical Behavior and Biofuel Properties of Sewage Sludge Pyrolysis."

[62] Y. Lin *et al.*, "Co-pyrolysis kinetics of sewage sludge and oil shale thermal decomposition using TGA – FTIR analysis," *ENERGY Convers. Manag.*, vol. 118, pp. 345–352, 2016.

[63] Y. W. Huang, M. Q. Chen, and H. F. Luo, "Nonisothermal torrefaction kinetics of sewage sludge using the simplified distributed activation energy model," *Chem. Eng. J.*, vol. 298, pp.

154–161, 2016.

[64] V. Strezov, T. J. Evans, T. Kan, V. Strezov, and T. Evans, “Thermochemical behaviour of sewage sludge during its slow pyrolysis Thermochemical behaviour of sewage sludge during its slow pyrolysis,” no. August, 2015.

[65] A. Bhavanam and R. C. Sastry, “Bioresource Technology Kinetic study of solid waste pyrolysis using distributed activation energy model,” *Bioresour. Technol.*, 2014.

[66] R. Han, C. Zhao, J. Liu, A. Chen, and H. Wang, “Bioresource Technology Thermal characterization and syngas production from the pyrolysis of biophysical dried and traditional thermal dried sewage sludge,” *Bioresour. Technol.*, vol. 198, pp. 276–282, 2015.

[67] J. Cao, P. Shi, X. Zhao, X. Wei, and T. Takarada, “Catalytic reforming of volatiles and nitrogen compounds from sewage sludge pyrolysis to clean hydrogen and synthetic gas over a nickel catalyst,” *Fuel Process. Technol.*, vol. 123, pp. 34–40, 2014.

[68] M. B. Folgueras, M. Alonso, and R. M. Díaz, “In fl uence of sewage sludge treatment on pyrolysis and combustion of dry sludge,” pp. 1–10, 2013.

[69] W. Xiaohua and J. Jiancheng, “Energy Procedia Effect of Heating Rate on the Municipal Sewage Sludge Pyrolysis Character,” vol. 0, no. 2011, pp. 0–4, 2012.

[70] Z. Lai, X. Ma, Y. Tang, and H. Lin, “Thermogravimetric analysis of the thermal decomposition of MSW in N 2 , CO 2 and CO 2 / N 2 atmospheres,” *Fuel Process. Technol.*, vol. 102, pp. 18–23, 2012.

[71] S. Werle and R. K. Wilk, “A review of methods for the thermal utilization of sewage sludge: The Polish perspective,” *Renew. Energy*, vol. 35, no. 9, pp. 1914–1919, 2010.

[72] A. V. Bridgwater, “Review of fast pyrolysis of biomass and product upgrading,” *Biomass and Bioenergy*, vol. 38, pp. 68–94, 2012.

[73] G. W. Huber and R. C. Brown, “Prospects and Challenges of Pyrolysis Technologies for Biomass Conversion,” *Energy Technol.*, vol. 5, no. 1, pp. 5–6, 2017.

[74] M. Jahirul, M. Rasul, A. Chowdhury, and N. Ashwath, “Biofuels Production through Biomass Pyrolysis —A Technological Review,” *Energies*, vol. 5, no. 12, pp. 4952–5001, Nov. 2012.

[75] D. Mohan, C. U. Pittman, and P. H. Steele, “Pyrolysis of wood/biomass for bio-oil: A critical review,” *Energy and Fuels*, vol. 20, no. 3, pp. 848–889, 2006.

[76] R. O. Arazo, D. A. D. Genuino, M. D. G. de Luna, and S. C. Capareda, “Bio-oil production from dry sewage sludge by fast pyrolysis in an electrically-heated fluidized bed reactor,” *Sustain. Environ. Res.*, vol. 27, no. 1, pp. 7–14, 2017.

[77] P. Zhou, S. Xiong, Y. Zhang, H. Jiang, Y. Chi, and L. Li, “Study on the nitrogen transformation during the primary pyrolysis of sewage sludge by Py-GC/MS and Py-FTIR,” *Int. J. Hydrogen Energy*, vol. 42, no. 29, pp. 18181–18188, 2017.

[78] N. Gao, C. Quan, B. Liu, Z. Li, C. Wu, and A. Li, “Continuous Pyrolysis of Sewage Sludge in a Screw-Feeding Reactor: Products

Characterization and Ecological Risk Assessment of Heavy Metals," *Energy and Fuels*, vol. 31, no. 5, pp. 5063–5072, 2017.

[79] J. Zhang, W. Zuo, Y. Tian, L. Chen, L. Yin, and J. Zhang, "Sulfur Transformation during Microwave and Conventional Pyrolysis of Sewage Sludge," *Environ. Sci. Technol.*, vol. 51, no. 1, pp. 709–717, Jan. 2017.

[80] H. Fan and K. He, "Fast Pyrolysis of Sewage Sludge in a Curie-Point Pyrolyzer: The Case of Sludge in the City of Shanghai, China," *Energy & Fuels*, p. acs.energyfuels.5b02235, Jan. 2016.

[81] "Slow pyrolysis of pre-dried sewage sludge ," *Chemical Papers* , vol. 70. p. 1479, 2016.

[82] L. Wei, L. Wen, T. Yang, and N. Zhang, "Nitrogen Transformation during Sewage Sludge Pyrolysis," *Energy & Fuels*, vol. 29, no. 8, pp. 5088–5094, Aug. 2015.

[83] Y. Sun *et al.*, "Effects of temperature and composite alumina on pyrolysis of sewage sludge," *J. Environ. Sci.*, vol. 30, pp. 1–8, Apr. 2015.

[84] H. Fan, H. Zhou, and J. Wang, "Pyrolysis of municipal sewage sludges in a slowly heating and gas sweeping fixed-bed reactor," *Energy Convers. Manag.*, vol. 88, pp. 1151–1158, Dec. 2014.

[85] Q. Xie *et al.*, "Fast microwave-assisted catalytic pyrolysis of sewage sludge for bio-oil production," *Bioresour. Technol.*, vol. 172, pp. 162–168, Nov. 2014.

[86] C. Di Blasi, "Modeling chemical and physical processes of wood and biomass pyrolysis," *Prog. Energy Combust. Sci.*, vol. 34, no. 1,

pp. 47–90, Feb. 2008.

[87] X. Y. Zhang and M. Q. Chen, “A comparison of isothermal with nonisothermal drying kinetics of municipal sewage sludge,” *J. Therm. Anal. Calorim.*, vol. 123, no. 1, pp. 665–673, Jan. 2016.

[88] R. P. Liu, R. Yao, and B. Bin Dong, “Effects of Metal Oxides during Pyrolysis Sludge by Kinetic Analysis,” *Adv. Mater. Res.*, vol. 864–867, pp. 1854–1858, Dec. 2013.

[89] Z. Lai, X. Ma, Y. Tang, and H. Lin, “A study on municipal solid waste (MSW) combustion in N2/O2 and CO2/O2 atmosphere from the perspective of TGA,” *Energy*, vol. 36, no. 2, pp. 819–824, Feb. 2011.

[90] J. Shao, R. Yan, H. Chen, H. Yang, and D. H. Lee, “Catalytic effect of metal oxides on pyrolysis of sewage sludge,” *Fuel Process. Technol.*, vol. 91, no. 9, pp. 1113–1118, Sep. 2010.

[91] A. G. Barneto, J. A. Carmona, J. E. M. Alfonso, and J. D. Blanco, “Kinetic models based in biomass components for the combustion and pyrolysis of sewage sludge and its compost,” *J. Anal. Appl. Pyrolysis*, vol. 86, no. 1, pp. 108–114, Sep. 2009.

[92] A. R. Mohamed, Z. Hamzah, M. Z. M. Daud, and Z. Zakaria, “The Effects of Holding Time and the Sweeping Nitrogen Gas Flowrates on the Pyrolysis of EFB using a Fixed–Bed Reactor,” *Procedia Eng.*, vol. 53, pp. 185–191, Jan. 2013.

[93] M. Auta, L. M. Ern, and B. H. Hameed, “Fixed-bed catalytic and non-catalytic empty fruit bunch biomass pyrolysis,” *J. Anal. Appl. Pyrolysis*, vol. 107, pp. 67–72, May 2014.

[94] K. Murata, Y. Liu, M. Inaba, and I. Takahara, “Catalytic fast pyrolysis of jatropha wastes,” *J. Anal. Appl. Pyrolysis*, vol. 94, pp. 75–82, Mar. 2012.

[95] D. R. Nhuchhen and P. Abdul Salam, “Estimation of higher heating value of biomass from proximate analysis: A new approach,” *Fuel*, vol. 99, pp. 55–63, Sep. 2012.

[96] H. Günzler and H.-U. Gremlich, *IR spectroscopy : an introduction*. Wiley-VCH, 2002.

[97] P. Inc, “Thermogravimetric Analysis (TGA) The Thermogravimetric Instrument Family.”

[98] R. Ebrahimi-Kahrizsangi and M. H. Abbasi, “Evaluation of reliability of Coats-Redfern method for kinetic analysis of non-isothermal TGA,” *Trans. Nonferrous Met. Soc. China*, vol. 18, no. 1, pp. 217–221, Feb. 2008.

[99] A. K. and and D. R. Flanagan, “Complementary Use of Model-Free and Modelistic Methods in the Analysis of Solid-State Kinetics,” 2005.

[100] D. Zhao, K. Chen, F. Yang, G. Feng, Y. Sun, and Y. Dai, “Thermal degradation kinetics and heat properties of cellulosic cigarette paper: influence of potassium carboxylate as combustion improver,” *Cellulose*, vol. 20, no. 6, pp. 3205–3217, Dec. 2013.

[101] S. Völker and T. Rieckmann, “Thermokinetic investigation of cellulose pyrolysis - Impact of initial and final mass on kinetic results,” *J. Anal. Appl. Pyrolysis*, vol. 62, no. 2, pp. 165–177, 2002.

[102] Y. S. Kim, Y. S. Kim, and S. H. Kim, “Investigation of

Thermodynamic Parameters in the Thermal Decomposition of Plastic Waste−Waste Lube Oil Compounds," *Environ. Sci. Technol.*, vol. 44, no. 13, pp. 5313–5317, Jul. 2010.

[103] I. Fonts, M. Azuara, G. Gea, and M. B. Murillo, "Study of the pyrolysis liquids obtained from different sewage sludge," *J. Anal. Appl. Pyrolysis*, vol. 85, no. 1–2, pp. 184–191, May 2009.

[104] X. Xu *et al.*, "Co-pyrolysis characteristics of municipal sewage sludge and hazelnut shell by TG-DTG-MS and residue analysis," *Waste Manag.*, vol. 62, pp. 91–100, Apr. 2017.

[105] A. Demirbaş, "Calculation of higher heating values of biomass fuels," *Fuel*, vol. 76, no. 5, pp. 431–434, Apr. 1997.

[106] J.-P. Cao *et al.*, "Nitrogen transformations during fast pyrolysis of sewage sludge," *Fuel*, vol. 104, pp. 1–6, Feb. 2013.

[107] W. Zuo, B. Jin, Y. Huang, and Y. Sun, "Characterization of top phase oil obtained from co-pyrolysis of sewage sludge and poplar sawdust," *Environ. Sci. Pollut. Res.*, vol. 21, no. 16, pp. 9717–9726, Aug. 2014.

[108] M. Jeguirim and G. Trouvé, "Pyrolysis characteristics and kinetics of Arundo donax using thermogravimetric analysis," *Bioresour. Technol.*, vol. 100, no. 17, pp. 4026–4031, Sep. 2009.

[109] D. Vamvuka, E. Kakaras, E. Kastanaki, and P. Grammelis, "Pyrolysis characteristics and kinetics of biomass residuals mixtures with lignite☆," *Fuel*, vol. 82, no. 15–17, pp. 1949–1960, Oct. 2003.

[110] M. A. Lopez-Velazquez, V. Santes, J. Balmaseda, and E. Torres-

Garcia, “Pyrolysis of orange waste: A thermo-kinetic study,” *J. Anal. Appl. Pyrolysis*, vol. 99, pp. 170–177, Jan. 2013.

[111] A. K. Sadhukhan, P. Gupta, T. Goyal, and R. K. Saha, “Modelling of pyrolysis of coal–biomass blends using thermogravimetric analysis,” *Bioresour. Technol.*, vol. 99, no. 17, pp. 8022–8026, Nov. 2008.

[112] J. Madarász, P. P. Varga, and G. Pokol, “Evolved gas analyses (TG/DTA–MS and TG–FTIR) on dehydration and pyrolysis of magnesium nitrate hexahydrate in air and nitrogen,” *J. Anal. Appl. Pyrolysis*, vol. 79, no. 1–2, pp. 475–478, May 2007.

[113] A. Demirbaş, “Mechanisms of liquefaction and pyrolysis reactions of biomass,” *Energy Convers. Manag.*, vol. 41, no. 6, pp. 633–646, Apr. 2000.

[114] X. Y. Zhang and M. Q. Chen, “A comparison of isothermal with nonisothermal drying kinetics of municipal sewage sludge,” *J. Therm. Anal. Calorim.*, vol. 123, no. 1, pp. 665–673, Jan. 2016.

[115] B. V. Babu and A. S. Chaurasia, “Parametric study of thermal and thermodynamic properties on pyrolysis of biomass in thermally thick regime,” *Energy Convers. Manag.*, vol. 45, no. 1, pp. 53–72, Jan. 2004.

[116] T. Damartzis, D. Vamvuka, S. Sfakiotakis, and A. Zabaniotou, “Thermal degradation studies and kinetic modeling of cardoon (Cynara cardunculus) pyrolysis using thermogravimetric analysis (TGA),” *Bioresour. Technol.*, vol. 102, no. 10, pp. 6230–6238, May 2011.

[117] Y. S. Kim, Y. S. Kim, and S. H. Kim, “Investigation of Thermodynamic Parameters in the Thermal Decomposition of Plastic Waste−Waste Lube Oil Compounds,” *Environ. Sci. Technol.*, vol. 44, no. 13, pp. 5313–5317, Jul. 2010.

[118] M. Baratieri, P. Baggio, L. Fiori, and M. Grigiante, “Biomass as an energy source: Thermodynamic constraints on the performance of the conversion process,” *Bioresour. Technol.*, vol. 99, no. 15, pp. 7063–7073, Oct. 2008.

[119] Y. Xu and B. Chen, “Investigation of thermodynamic parameters in the pyrolysis conversion of biomass and manure to biochars using thermogravimetric analysis,” *Bioresour. Technol.*, vol. 146, pp. 485–493, Oct. 2013.

[120] J. Alvarez, M. Amutio, G. Lopez, J. Bilbao, and M. Olazar, “Fast co-pyrolysis of sewage sludge and lignocellulosic biomass in a conical spouted bed reactor,” *Fuel*, vol. 159, pp. 810–818, Nov. 2015.